UNIVERSIDADE DE LISBOA

FACULDADE DE CIÊNCIAS

DEPARTAMENTO DE BIOLOGIA ANIMAL

Role of Tropomyosin2 in cell proliferation and survival of *Drosophila melanogaster*

Filipe Paulos e Cruz Oliveira Viegas

Mestrado em Biologia Evolutiva e do Desenvolvimento

Dissertação orientada por:
Doutora Florence Janody, IGC
Doutora Gabriela Rodrigues, FCUL

2016

Acknowledgements

The work before you would not be the same, or even exist, if not for several people. Though many deserve my gratitude, I can only thank so many without making this too long.

First of all, I'd like to thank my supervisor, Florence. Thank you for this amazing opportunity. I wholeheartedly thank you for accepting me in your laboratory and providing me with this enticing and really cool work. Thank you for your patience and perseverance, they did not go unnoticed. Most of all, thank you for teaching me so much.

I'd also like to thank the members of the Actin dynamics Lab that accompanied me throughout this journey: Catarina, Sandra, Prachii, Margarida and Clara. Your help and friendship was crucial to my work and learning process. I'm very grateful.

To Sónia, Liliana, Pedro and Gaston: you may not realize it, but you helped. A lot. I can't thank you enough for your support and companionship.

To Nuno and Ania. Without you, I'd still be struggling with the microscopes. Thank you so much for your help.

To Professor Gabriela. For accepting me as her external student but most of all for being a wonderful and inspiring teacher throughout my Biology course and masters. You are part of the reason I love developmental biology and for that, I can't thank you enough.

The other part responsible for my love of developmental biology would be Professor Solveig. From the first few lessons of animal developmental biology, I knew exactly what I wanted to dedicate my career to. It wasn't just that development is really, really cool and fascinating. It was the way you taught it. Thank you.

To my family and closest friends. Thank you for your support, it's what got me through this journey with my sanity (somewhat) intact. I'm sorry for neglecting you while writing this.

Last of all, Ana. Without you none of this would be possible. Thank you for everything.

Abstract

The Actin cytoskeleton is a vital cell component that controls a large number of cellular processes, including cell shape, mobility and intracellular transport. The cytoskeleton also transmits external forces into signaling activity, such as Hippo pathway signaling, which controls tissue growth and cell fate decision during development and adult homeostasis. Tropomyosins belong to a highly conserved and diverse family of actin-binding proteins (ABPs), which stabilize and regulate the functional diversity of actin filaments, by mediating their interaction with other ABPs Additionally, Tropomyosins contribute to tumorigenesis, though the mechanisms remain unclear. In our lab, Tropomyosin2 (*tm2*) was identified as an ABP that seems to restrict *Drosophila* wing imaginal disc growth. This presented the opportunity to further investigate if *tm2* restricts wing disc growth and to identify if the underlying mechanism could be Hippo pathway activity regulation. *tm2* downregulation promotes larval wing disc and adult wing overgrowth. The solicited overgrowth displayed phenotypic variability, from no apparent overgrowth to heavily affected tissue size and morphology. The effect of *tm2* downregulation on F-actin levels also seems to be linked to this phenotypic penetrance effect as discs with no overgrowth appeared to have less actin while those with overgrowth had F-actin accumulation. Moreover, when *tm2* downregulation induced tissue overgrowth, there is upregulation of Hippo target genes. Taken together, these observations suggest that *tm2* could be necessary to prevent wing disc overgrowth by regulating F-actin levels and Hippo pathway activity. In *Drosophila*, Tropomyosin had yet to be linked to tissue growth, which suggests a novel regulatory function of *tm2* *in vivo* and while the actin cytoskeleton is known to regulate Hippo pathway activity, this work present novel evidences for a possible role of Tropomyosins intervening in this regulation. Finally, I hypothesize that *tm2* could be necessary to translate external cues, such as mechanical force, into wing disc growth termination by triggering Hippo pathway activity.

Key-words: Actin cytoskeleton; Hippo pathway; Tropomyosin; Growth control; *Drosophila melanogaster*

Sumário

O citoesqueleto de actina é responsável por um grande número de processos celulares, tais como a forma e a mobilidade celular, o transporte intracelular, a citocinese. Este também traduz forças mecânicas exteriores à célula em sinalização bioquímica, modulando a expressão genética. O citoesqueleto de actina é formado por filamentos de actina (F-actina) que por sua vez são compostos por monómeros de actina globular (G-actina) e é a organização destes filamentos em arquiteturas especializadas e distintas que definem as propriedades mecânicas destas. A organização e função de diferentes arquiteturas de F-actina depende da interação e ligação destas com proteínas especializadas, as *actin binding proteins* – ABPs que estão divididas em famílias consoante a sua função. Estas proteínas ao interagirem com a F-actina, levam à formação de redes de F-actina distintas e especializadas. Uma família particular de ABPs são as Tropomiosinas.

As Tropomiosinas são uma família conservada à qual é atribuída um papel fundamental na regulação funcional de filamentos de actina em células musculares e não-musculares. As proteínas desta família regulam uma larga variedade de funcionalidades do citoesqueleto ao recrutar, de modo específico, outras ABPs para a F-actina. Os mamíferos possuem quatro genes de Tropomiosina – TPM1, TPM2, TPM3 e TPM4 – que, dão origem a mais de 40 isoformas através de *splicing* alternativo, mas apenas metade destas estão confirmadas. Estas isoformas são normalmente divididas em duas categorias, segundo o seu peso molecular: as *high molecular weight* (HMW) e as *low molecular weight* (LMW). A *Drosophila melanogaster* possui apenas dois genes de Tropomiosina – *tm1* e *tm2*. A *tm2* dá origem à isoforma Tm2-A/B e à isoforma Tm2-C. Ao regular a funcionalidade do citoesqueleto, as Tropomiosinas tornam-se essenciais ao correto funcionamento celular. A sua importância, leva a que as Tropomiosinas estejam associadas a várias patologias humanas, uma das quais o cancro. Na verdade, diversos estudos já correlacionaram alterações na expressão genética de Tropomiosinas com fenótipos em células cancerígenas. Curiosamente, os mesmos estudos encontraram que existem isoformas especificas que se encontram altamente expressas em células cancerígenas, enquanto outras isoformas se encontram silenciadas.

Num estudo de *microarray* para ABPs desreguladas numa linha celular com transformação induzível, bem como em amostras tumorais de pacientes humanos, o Laboratório *Actin Dynamics* identificou que a TPM2 se encontrava sub-expressa em ambos os casos. Em *Drosophila*, a *tm2* mostrou ser necessária para prevenir o crescimento excessivo em discos imaginais de asa. Estas observações sugerem que a *tm2* pode ter um papel em restringir a proliferação celular, tal como acontece em Tropomiosinas HMW humanas. Para além disso, a proliferação celular desregulada e excessiva é uma das principais características em tumores.

Um dos muitos papeis do citoesqueleto de actina passa por regular o crescimento de tecidos e órgãos através da via de sinalização de supressão de tumores Hippo. Esta via de sinalização é constituída por uma cascata de cinases composta por Hippo (Hpo), Salvador (Sav), Mob as Tumor Supressor (Mats) e Warts (Wts). Hpo fosforila Wts, que por sua vez fosforila e inativa Yorkie (Yki). Yki é um cofator de transcrição cuja atividade leva à expressão de genes de proliferação e anti-apoptose, levando assim ao crescimento de tecidos e órgãos. Deste modo, quando a via de sinalização Hippo não está ativa, Yki está no núcleo a promover a proliferação celular e a sobrevivência. Quando a via Hippo está ativa, Wts fosforila Yki e impede este de entrar no núcleo e levar a expressão dos seus genes-alvo.

Visto que o citoesqueleto regula a atividade desta via de sinalização e que as Tropomiosinas regulam a funcionalidade do citoesqueleto, existe a possibilidade de *tm2* restrinja o crescimento de tecidos por regular a atividade da via de sinalização Hippo. Assim, o presente estudo pretende validar o papel da *tm2* no crescimento de discos imaginais de asa de *Drosophila* tal como averiguar se a restrição do crescimento se faz através da via de sinalização Hippo.

De modo a validar o papel que a *tm2* tem em limitar o crescimento em discos imaginais de asa e em asas adultas, foram utilizadas duas linhas de moscas com transgenes que expressam RNAi: a linha *tm2*-IR^{JF01095} e a linha *tm2*-IR^{HMS02260}. Os resultados parecem indicar que a sub-expressão de *tm2* levou a um aumento significativo no tamanho do domínio distal do disco de asa e de asas adultas. Surpreendentemente, o crescimento excessivo em discos que sub-expressam *tm2* não foi igual em todos os discos, levantando assim a possibilidade da *tm2* apenas contribuir para a restrição do crescimento no fim do desenvolvimento do disco, quando este para de crescer. Assim, a *tm2* restringe o crescimento excessivo na asa. Adicionalmente, quando a sub-expressão de *tm2* leva a crescimento excessivo, este é acompanhado de um aumento nos níveis de F-actina, mas quando não há crescimento excessivo existe um decréscimo nos níveis de F-actina. A sub-expressão de *tm2* também levou ao aumento do nível de *expanded, four-jointed* e Wingless, todos genes-alvo da atividade de Yki, indicando assim que *tm2* contribui para limitar a expressão de alvos transcricionais de Yki.

Para além destes resultados, também foi feita uma comparação entre os genes de Tropomiosina humanos e de *Drosophila*. Nesta análise foram comparados os exões codificantes de todos os genes humanos (TPM1, TPM2, TPM3 e TPM4) com cada exão dos genes de *Drosophila* (*tm1* e *tm2*). Esta análise permitiu verificar que as isoformas de *tm2* parecem ser mais comparáveis às Tropomiosinas humanas HMW do que às LMW.

Estes resultados parecem sugerir que a *tm2* pode ser responsável por restringir o crescimento excessivo no disco de asa de *Drosophila*. Adicionalmente, parece também haver um efeito oposto no que toca à regulação dos níveis de F-actina entre as duas isoformas da *tm2*, a Tm2-A/B e a Tm2-C. Este efeito provavelmente é devido a uma regulação diferencial de ABPs e o facto de haver efeitos opostos vai de encontro a estudos prévios que constataram que diferentes isoformas do mesmo gene de Tropomiosina podem ter efeitos distintos na regulação de ABPs.

No entanto, é provável que o papel que a isoforma Tm2-A/B tem em prevenir a acumulação excessiva de F-actina e em regular o crescimento da asa estejam ligados, o que vai de encontro com o facto de que o citoesqueleto de actina regula a atividade da via de sinalização Hippo. Para além disso, a Tm2-A/B parece ter um papel em regular a atividade transcricional de Yki.

Assim, uma rede de F-actina definida pela presença de Tm2-A/B poderá receber informação exterior e levando à regulação da via de sinalização Hippo de modo a controlar a atividade transcricional de Yki, parando assim o crescimento no fim do desenvolvimento do disco de asa de *Drosophila*. Tendo em conta que um dos papeis centrais do citoesqueleto de actina é mediar e contribuir para a geração de forças mecânicas no ambiente celular, estas mesmas forças poderão ser persentidas pela rede de F-actina contendo Tm2-A/B e traduzidas em regulação da atividade da via de sinalização Hippo. Deste modo, quando o disco imaginal da asa se encontra a desenvolver, esta rede de F-actina não afeta o crescimento e a via de sinalização Hippo está inativa, permitindo assim que os tecidos cresçam. Mais tarde, à medida que os tecidos crescem, existe uma acumulação de forças compressivas que são persentidas pela rede de F-actina que contém Tm2-A/B, ativando assim a via de sinalização Hippo e consequente cessar do crescimento.

Palavras-chave: Citoesqueleto de actina; Via de sinalização Hippo; Tropomiosina; Controlo de crescimento; *Drosophila melanogaster*

Table of Contents

Figure Index

Table Index

I Introduction

1. The Actin Cytoskeleton

The ability of animal cells to change their shape, move and divide allow them to adapt to their environment. The mechanisms behind these structural changes rely on a complex network of protein filaments in the cytoplasm, the actin cytoskeleton that organize into a wide range of complex structures[1,2].

1.1 Actin binding proteins drive F-actin dynamics

In cells, actin exists in two forms: globular actin (G-actin) monomers and filamentous actin (F-actin) polymers, assembled from G-actin monomers[1,3] . Actin cytoskeletal dynamics are established by the homeostatic balance between these two forms, where ATP-bound G-actin is added to the fast-growing barbed-end (+) of F-actin while ADP-bound G-actin dissociates from the slow-growing pointed-end (-)[3,4]. This process, known as "treadmilling", is spatiotemporally regulated by a plethora of different actin-binding proteins (ABPs)[3,4] (Fig.1). By promoting and controlling F-actin nucleation, dissociation, bundling and crosslinking, ABPs are crucial in determining architectures of functionally distinct F-actin networks which make up essential cytoskeletal structures such as filopodia, lamellipodia, stress fibers and the actin cortex[1,4] (Fig.1).
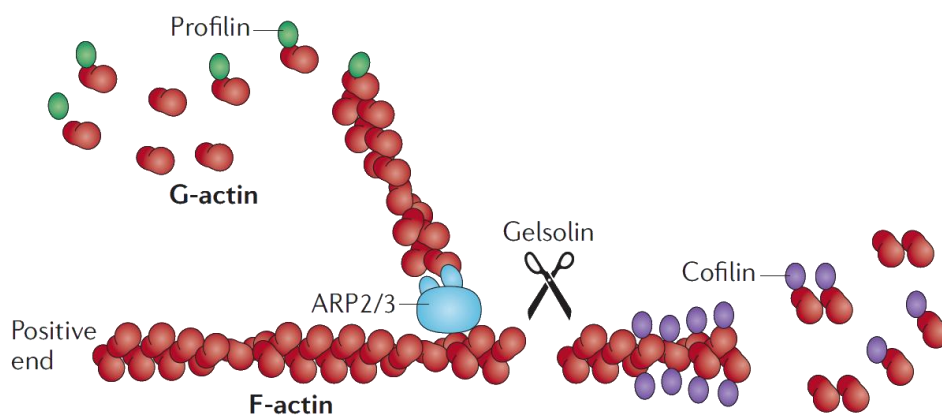
Figure 1 | Actin dynamics regulation by ABPs[5]

The assembly of F-actin networks relies mainly on nucleation and elongation factors, such as Formins and the Arp2/3 complex[1,3]. Formins mediate the assembly of unbranched actin networks by stabilizing an actin dimer polymerization nucleus and promoting its elongation at the barbed-end.

The Arp2/3 complex mediates the formation of branched actin networks[1,6,7]. When activated, Arp2/3 nucleates new actin filaments by binding to the side of a pre-existing filament[6]. Capping Protein (CP) forms a protein cap that arrests actin polymerization by preventing further addition and loss of actin monomers[3].

The main contributors towards disassembly of F-actin networks are the ADF/Cofilin family of ABPs[3,4,8]. ADF/Cofilin is a disassembly factor that uses fragmentation or severing to break down actin organizations[1]. Therefore, ADF/Cofilin-mediated disassembly facilitates network turnover thus contributing to higher-order structures like lamellipodia[1].

A special group of ABPs are the members of the myosin superfamily[4,9], which are molecular motors responsible for global cell contraction and tension at focal adhesion sites. Myosins have also been recently identified as F-actin disassembly agents, where their contractile function causes filament buckling and fragmentation[1].

The above-mentioned ABPs are some of the most studied for proper cytoskeleton architecture. One of the ABP families that was not mentioned above is the Tropomyosin family, pervasive in actin cytoskeletal function[10-12].

2. Tropomyosin – Regulators of Actin Cytoskeletal Function

Tropomyosins are conserved ABPs that were first described as regulators of skeletal muscle contraction[13] and for a long time they were thought to only exist associated to the contractile apparatus in muscle cells. However, Tropomyosins were recently described as having a key role in regulating the function of actin filaments in both muscle and non-muscle cells[14,15]. In fact, more complex roles for Tropomyosins in non-muscle cells have recently emerged, demonstrating that Tropomyosins regulate a wide range of cytoskeletal functions by differentially recruiting other ABPs on F-actin. Still, the precise roles of Tropomyosin in non-muscle cells are far from resolved[11,12].

2.1 Gene and protein structure

Mammals have four Tropomyosin genes – TPM1, TPM2, TPM3, TPM4[11,16]. Mainly through the use of alternative splicing, each gene gives rise to a variable number of isoforms, expressed in both muscle and non-muscle cells, with over 20 Tropomyosin isoforms identified by RT-PCR. However, the existence of only half these isoforms have been confirmed at the protein level or with Northern blots[16].

Exon organization of the four mammalian Tropomyosin genes is extremely similar, as is their sequence homology[16,17]. Exons 3,4,5,7 and 8 have a high degree of sequence conservation and are present in all mammalian isoforms (Fig.2) while exons 1a/1b, 2a/2b, 6a/6b, 9a/9b/9c/9d have a much lower degree of conservation among the different TPM genes. The presence of exons 1a/1b, 2a/2b, 6a/6b, 9a/9b/9c/9d is the source of isoform variability and their lower sequence conservation is the main source of divergence between isoforms from different genes[18-20] (Fig.2). The isoforms generated this way are usually classified by their molecular weight as either low molecular weight (LMW) or high molecular weight (HMW)[11]. LMW isoforms are approximately 248 amino acids in length and their N-termini contains exon 1b but not 2a or 2b, while HMW isoforms have an approximate length of 284 amino acids. and their N-termini contains exon 1a and either 2a or 2b[11,18].
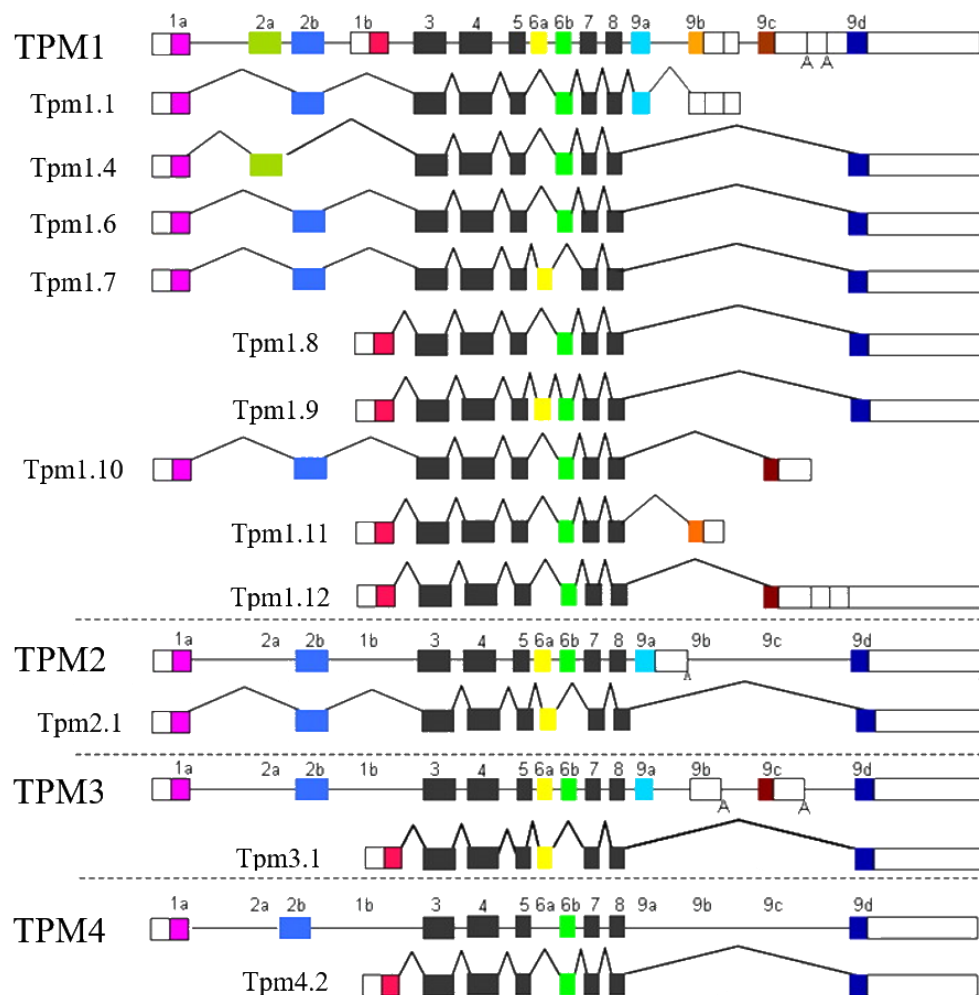
Figure 2 | Mammalian TPM exon structure[11,18]

Black – exons present in all isoforms of all genes. **Colored** – alternatively spliced exons.

While not as extensively studied as mammalian Tropomyosins, there has been a recent surge of studies concerning cytoskeletal Tropomyosin function in the fruit fly[20-24]. Unlike mammals, *Drosophila melanogaster* has two Tropomyosin genes – *tm1* and *tm2* and bioinformatics analyses predict 17 isoforms for *tm1* and 6 isoforms for *tm2*[25,26]. *tm2* has 4 coding exons, which give rise to six splice variants that vary in 5' and 3' UTR as well as in coding exon composition in the case of splice variant C (Fig.3). However, these six splice variants give rise to only two different proteins – splice variants A, B, E, F and G all give rise to isoform Tm2-A/B and splice variant C gives rise to isoform Tm2-C. Both isoforms differ only in the use of exon 3 or 4 – Tm2-A/B uses exons 1,2 and 4 while Tm2-C uses exons 1,2,3 (Fig.3).
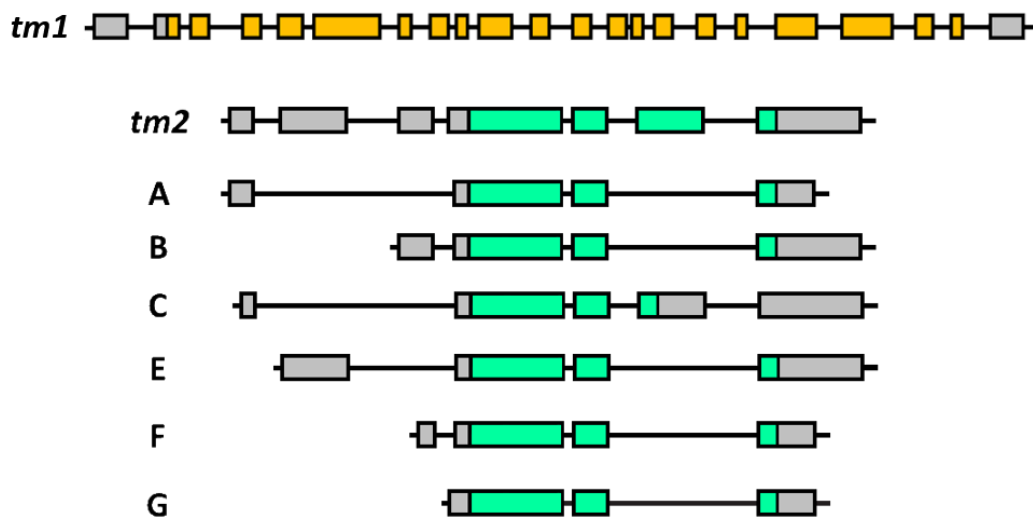
Figure 3 | Exon structure of *Drosophila* Tropomyosin genes

A-G – Predicted **s**plice variants of *Drosophila tm2*. **Grey –** Untranslated regions (UTR). **Colored** – Coding exons.

2.2 Tropomyosins regulate F-actin dynamics

Tropomyosin proteins form coiled-coil dimers linked end-to-end, which polymerize along the major grove of F-actin, cooperatively associating with actin[27]. In spite of this, individual interactions between tropomyosin molecules and F-actin are very weak[28,29].

Tropomyosins have been proposed to regulate actin dynamics by mediating the interaction of F-actin with ABPs, including the Arp2/3 complex, Formins, ADF/Cofilin, Myosin II, among others[11,30].

Several studies have reported Tropomyosins as inhibitors of Arp2/3-mediated actin nucleation[31-33]. Actin filaments decorated by HMW Tpm1.1 and Tmp1.7 exclude Arp2/3 while HMW Tpm1.6 and LMW Tpm1.8 reduce the branching properties of Arp2/3[31,33]. In a recent study, two LMW Tpm isoforms (1.8 and 1.9) were also shown to exclude Arp2/3 nucleation, though they were also excluded from populating Arp2/3-branched actin networks[34].

Formins have also been shown to interact with Tropomyosins[30]. *In vitro*, mammalian Tpm1.8 activates formin-mediated elongation while Tpm1.6 does so to a lesser extent[35]. Formins also recruit Tpm4.2 to actin filament arcs in osteosarcoma cells[36] and in budding yeast, which has only two tropomyosins (Tpm1p and Tm2p), Formin-nucleated F-actin recruits both Tropomyosins, thus enabling rapid filament elongation[37].

Tropomyosin has contrasting, isoform-specific effects on ADF/cofilin-mediated actin filament disassembly[11,12]. The stabilizing effects of Tropomyosins on filaments have been shown to protect against the effects of ADF/Cofilin as both proteins compete for binding on actin[11]. Thus, mammalian Tpm3.1 and *C. elegans* Tropomyosins (CeTMI, II, III, IV) have an antagonistic relationship with ADF/Cofilin in regulating F-actin dynamics[38]. In contrast, Tpm1.12, Tpm1.7, Tpm2.1 and Tpm4.2 have been reported to actively recruit ADF/Cofilin[11,30].

Finally, Tropomyosin regulation of Myosin activity has been extensively studied and more recently, Tropomyosins have been shown to have an isoform-specific impact on the activity and location of Myosins in many studies and organisms[11,12,30]. For example, in budding yeast one Tropomyosin (Tpm2p) prevents Myosin1p activity while the other (Tpm1p) promotes MyosinV activity[12]. In another case, Tpm3.1 recruits MyosinIIA but excludes Myosin1c from binding to F-actin in mouse adipocytes[12]. While not mentioned in detail, other ABPs such as Gelsolin, Tropomodulin, Caldesmon and Drebrin, are also regulated by Tropomyosin[11,30,39].

By regulating the activity of specific ABPs, Tropomyosins contribute towards the construction and maintenance of fundamental cytoskeletal structures [11,12,20].

2.3 Tropomyosins role in cell function

A significant body of work has established that Tropomyosins are vital for normal cell function[11,12]. Owing to a precise temporal expression and spatial distribution of Tropomyosin[11], they contribute to a wide variety of critical processes in the organism, including embryogenesis, morphogenesis, cell trafficking, glucose metabolism, cell biomechanics and muscle function[12].

Given the importance of Tropomyosins in cytoskeletal function and their contribution to major cell functions, Tropomyosins have been associated with human disease, from neuropathologies like Alzheimer's disease to cardiac and skeletal muscle diseases[11]. In addition, Tropomyosins have been directly and intimately linked to cancer progression[11,40,41].

3. *Drosophila* **Wing Imaginal Disc – *In vivo* Epithelial Model to Study Growth**

Drosophila melanogaster is one of the most used model organisms worldwide. *Drosophila* life-cycle consists of an embryonic stage, after which there are three larval stages L1, L2 and L3 followed by pupa formation, form which fully-formed adults emerge[42].

Imaginal discs are precursor epithelial tissues that develop during the larval stages and ultimately give rise to major adult structures such as legs, eyes or wings[43]. The wing imaginal disc is a bi-layered epithelial tissue consisting of a columnar monolayer epithelium with a characteristic apical-basolateral architecture[44], covered by a thin outer layer of squamous epithelium called the peripodial membrane[44].

The adult *Drosophila* wing stems from the wing imaginal disc, which contains about 40 cells in L1 larvae[44]. Until the final larval stage, cell divisions occur all over the wing disc and in the final larval stages, there are areas with different patterns of cell growth and division[44].

Throughout this process, wing discs proliferate to a final size of approximately 50,000 cells[43,44]. The size and shape of the adult wing is therefore predetermined by the patterns of cell growth, division and death in the disc[45].

In early larval stages, discs are subdivided into spatially distinct compartments where developmental signaling takes place[43,44]. This compartmentalized expression of patterning-genes makes the wing disc an appealing model to carry out gene-function assays. Thus, genes such as *engrailed* (*en*), *hedgehog* (*hh*), *wingless* (*wg*) and *apterous* (*ap*) (Fig.4) – which play key roles in Anterior-Posterior and Dorsal-Ventral patterning – are commonly used to drive gene expression using the Gal4-UAS system [43].
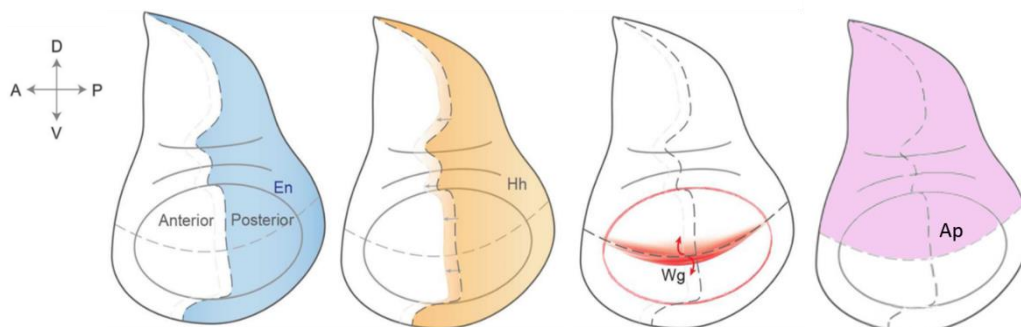

Figure 4 | Expression domains of key morphogenetic molecules in *Drosophila* wing imaginal disc during larval development[44]

4. Hippo Tumor Suppressor Pathway

The Hippo tumor suppressor pathway is a conserved regulator of organ size discovered in *Drosophila*[46-49]. The central component of this pathway is a kinase cascade composed by 4 tumor suppressors – Hippo (Hpo), Salvador (Sav), Warts (Wts) and Mob as Tumor Suppressor (Mats) – where the Hpo-Sav complex phosphorylates and activates the Wts-Mats kinase complex[46] (Fig.5). The downstream effectors of this kinase cascade is Yorkie (Yki), a transcriptional co-activator. When Hippo pathway is active, Wts directly phosphorylates and inactivates Yki. Being a transcriptional co-activator, Yki binds to transcription factors, such as Scalloped, to drive the expression of genes with roles in cell proliferation and survival[47,49]. Yki has been shown to function as an oncogene and its overexpression leads to over-proliferation and prevents cell death, thus phenocopying loss of Hippo signaling[47] (Fig.5).

Upstream regulation of Hpo kinase cascade activity is mainly directed by an apical complex consisting of Expanded (Ex), Merlin (Mer) and Kirba[47,48] (Fig.5). Independently from Mer and Kirba, Ex has been shown to regulate Yki activity independently of Hpo kinase cascade function, by directly binding and sequestering Yki in the cytoplasm[46]. Other upstream regulators are still emerging, such as the transmembrane protein Fat – an atypical cadherin involved in planar cell polarity (PCP) – which feeds into Hpo upstream regulation by localizing Ex[47] (Fig.5).

Mammals have two Hpo homologs (Mst1 and Mst2), one Sav homolog (Sav1), two Wts homologs (Lats1 and Lats2) and two Mats homologs (MOBKL1A and MOBKL1B). These proteins form a conserved kinase cassette that phosphorylates and inactivates the mammalian Yki homologs, YAP and TAZ[47,49] (Fig.5). There also appear to be tissue-specific requirements for pathway components, as YAP phosphorylation requires Mst1/2 in mouse liver but not in mouse embryonic fibroblasts[50].

Another particular aspect of the mammalian Hippo kinase cascade concerns the mechanism of YAP/TAZ inactivation. YAP nuclear-cytoplasmic translocation is seen as a major mechanism of YAP inactivation, though a recent report described an additional mode of regulation in which Lats1/2 primes YAP for subsequent degradation[51]. This mechanism is not conserved in Yki, revealing an important divergence between *Drosophila* and mammals[47]. Moreover, YAP/TAZ have more DNA-binding TF partners than Yki. Among these however, the TEAD/TEF TF family, homologs of *Drosophila* Sd protein, have emerged as the prime mediators of both YAP and TAZ function in Hippo signaling[47,48].

A remarkable feature of Hippo signaling is the fact it integrates growth control signals such as cell polarity, adhesion and contact, as well as mechanical forces have also been shown to affect Hippo signaling[49,53-55]. In fact, the actin cytoskeleton has been proposed as the link between mechanical force and Hippo pathway activity and the actin cytoskeleton is poised as a *de facto* regulator of Hippo pathway activity[54,55].
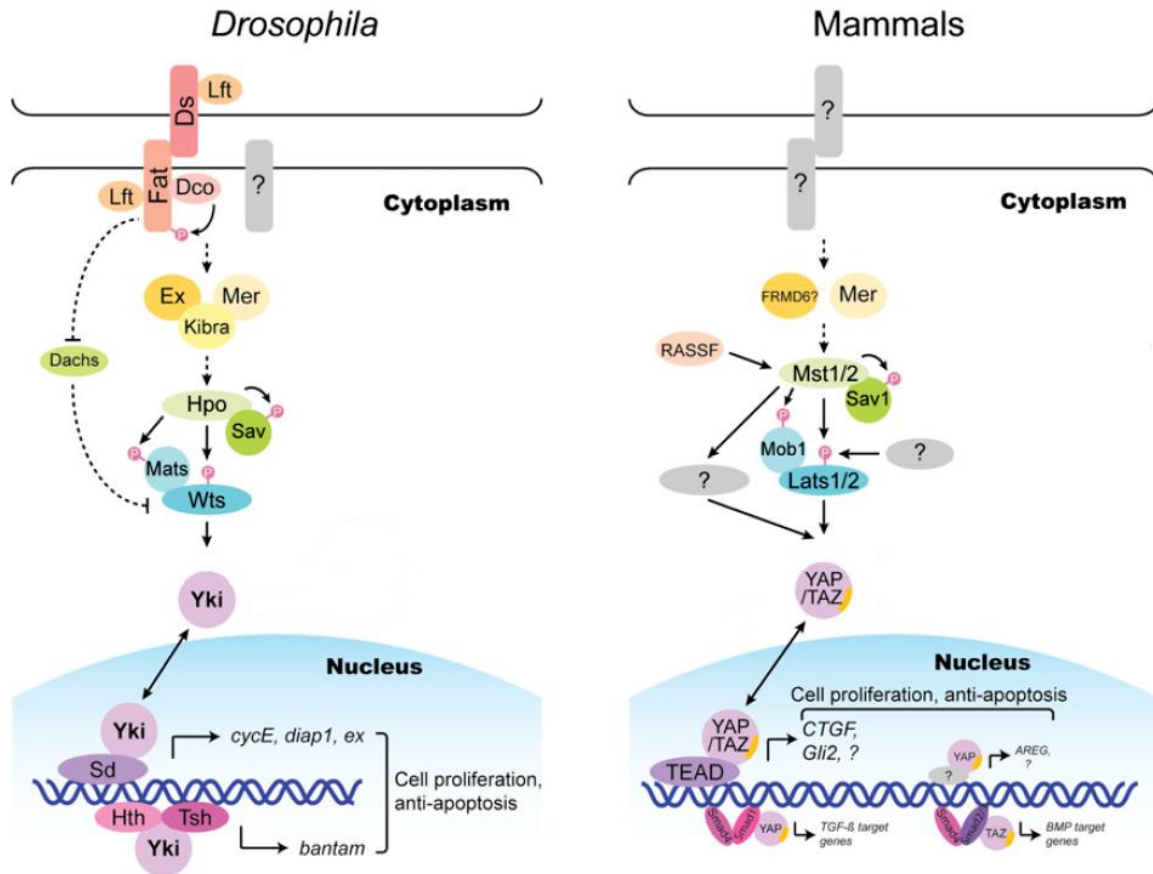
Figure 5 | Hippo pathway: similarities and differences between *Drosophila* and mammals[52]

4.1 Regulation of Hippo signaling by F-actin dynamics

Several reports, both in *Drosophila* and mammals, have demonstrated that the actin cytoskeleton does, in fact, play a role in controlling the oncogenic propensity of Yorkie[46].

The first reports showed that compromising the activity of F-actin regulators, such as CP and Capulet (Capt) – inhibitors of actin polymerization – as well as constitutive activity of Diaphanous (Dia) (actin-nucleating Formin) results in apical F-actin[56,57] accumulation (Fig.6). This, in turn, compromises Hippo pathway kinase-cascade activity, leading to ectopic Yki activation and tissue overgrowth. Moreover, F-actin accumulation is prevented by Hippo pathway at the kinase-cascade level, establishing a negative feedback loop where F-actin accumulation inhibits Hippo pathway activity and Hippo pathway inhibits F-actin accumulation, in a Yki-independent manner[56] (Fig.6).
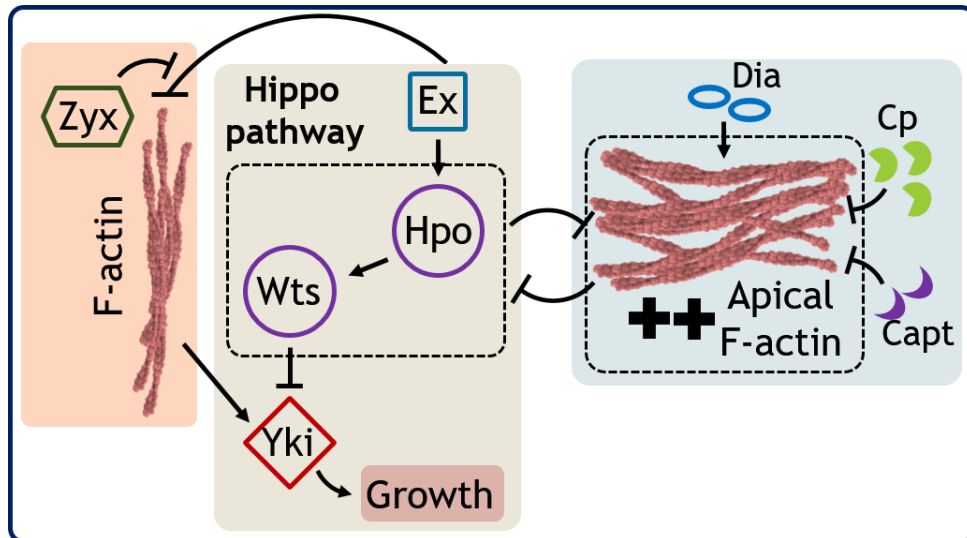
Figure 6 | Actin cytoskeleton regulation of Hippo pathway in *Drosophila*
Orange Box - Zyx promotes growth by antagonizing Ex-mediated F-actin regulation. **Blue box -** Actin filament networks where CP and Capt prevents and Dia promotes F-actin accumulation; **Beige box –** Simplified Hippo pathway schematic.

Another study shows that ABP Zyxin (Zyx) is directly involved in growth control by establishing a link between F-actin polymerization and Yki activity[58]. Zyx was shown to regulate Yki activity by antagonizing the effect Ex has on growth through F-actin accumulation, independently of Hippo kinase cascade activity (Fig.6). Another study in *Drosophila* has cytoskeletal tension modulate Yki activity by affecting MyoII activity[59].

Several studies in human cells have also linked F-actin dynamics to YAP/TAZ activity[49,53,54]. These studies generally report that an increase in F-actin seems to activate YAP/TAZ while destabilizing F-actin inhibits YAP/TAZ[49].

All together, these studies argue that different F-actin networks may translate upstream signaling and environmental cues into Hippo activity modulation, thereby regulating proliferation and cell survival.

5. Linking Tropomyosins and Tumorigenesis

5.1 Human Tropomyosins in cancer

Cancer cells show compromised developmental and genetic programs. These cells acquire a variety of alterations that allow them to sustain proliferative signaling, evade growth suppressors, activate invasion and metastasis, enable replicative immortality, induce angiogenesis and resist cell death[40,41,60].

Altered Tropomyosin expression profiles in transformed states have been observed *in vitro* and *in vivo,* where the expression of HMW Tropomyosin isoforms – Tpm1.4, Tpm1.6, Tpm1.7 and Tpm2.1 – is decreased[40]. HMW Tropomyosin downregulation has been observed in cells transformed with a wide variety of carcinogens and oncogenes[61] and *in vivo*, as tumor samples from breast, urinary bladder, central nervous system and colon have also shown a decrease in HMW Tropomyosin expression[40]. The loss of HMW Tropomyosins in transformed cells is thought to contribute to the improper assembly of microfilaments and adhesive structures, thereby contributing to the invasive and metastatic properties of cancer cells[40]. In addition, Tropomyosins are known to play a role in several cancer-associated cell phenotypes, such as anchorage-independent growth, apoptosis, cell division, migration and invasion[41].

The role Tropomyosin isoforms play in transformation is isoform specific, given that some isoforms can prevent transformation while others have the opposite effect[12,40,61]. More specifically, HMW Tmp2.1 and Tmp1.6 have been widely described as tumor suppressors[11,40,61]. Their expression is downregulated in transformed cells and tumor samples, as stated above, while restoring their expression prevented anchorage-independent growth, restored stress fiber formation and reduced cell motility – characteristics intimately tied with cell transformation[62,63].

On the other hand, Tmp3.1 expression is increased in all cancer cells of a large range of transformed cell lines, cultured cancer cells and patient tumor material[12,61] and contributes towards transformation and cell-motility. A recent report confirmed Tpm3.1 regulates cell proliferation and is requires for survival of neuroblastoma cells[61,64].

5.2 Tropomyosin and tissue growth in *Drosophila*

The study of Tropomyosins in *Drosophila* has mostly focused on the role this family of ABPs has in muscle contraction. Recently however, there have been a few studies concerning *Drosophila* Tropomyosins regarding their function in processes relevant to cancer[21,23,34].

Both *tm1* and *tm2* were seen to contribute in regulating chromosomal stability and nuclear integrity[21]. In a different study[23], a specific *tm1* isoform – Tm1-J – was found to localize to the mitotic spindle and promote proper chromosome segregation.

Another *tm1* isoform – Tm1-A – as well as Tm2-A/B (*tm2* isoform) were found surrounding the Golgi complex, where these isoforms influence cell-cycle progression. Genomic instability and cell-cycle misregulation are considered a key step in tumorigenesis and are considered characteristic of the cancer state[60]. Tm1-A has also been described to dynamically establish the border between the lamellipod and the lamellum in the leading edge of cells[34], structures which contribute to an invasive and metastatic cell state, common in transformed cells[1]. In spite of these observations and the impressive body of knowledge on Tropomyosins in cancer, further studies are still required to determine the mechanisms by which Tropomyosins differentially contribute to the transformed phenotype[40].

In a microarray screen for ABPs misregulated in pre-invasive Ductal Carcinoma *in situ* (DCIS) human tumor samples and in a Tamoxifen-induced MCF10A-ER-Src cell line, which recapitulates the multistep nature of breast cancer, the Actin Dynamics lab identified TPM2, which was downregulated in both cases. Strikingly, *Drosophila tm2* appeared to restrict growth of the distal part of the wing imaginal disc, as expressing a RNAi construct that target *tm2* to degradation, using the *nubbin*-Gal4 driver (*nub*-Gal4) that target gene expression in the distal wing imaginal disc domain[65] led to tissue overgrowth (Fig.7). Thus, these observations point towards a role of *tm2* in restricting proliferation, a feature shared with tumors[60].
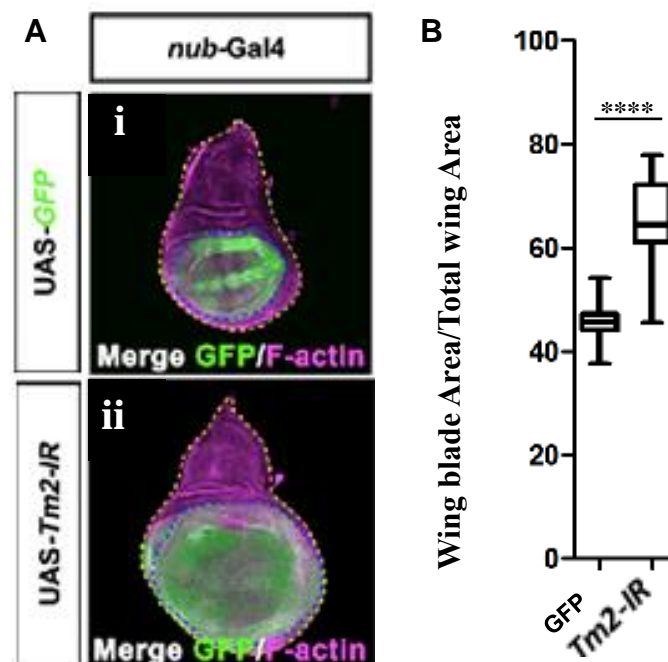
Figure 7 | Tm2 downregulation results in a significant increase in size of the wing blade
A – Standard confocal projections of wing imaginal discs from 3rd instar *Drosophila* larvae where *nub*-Gal4 is driving UAS-GFP (**i**), UAS-GFP and UAS-*tm2*-IR^{KK} (**ii**); *nub*-expressing domain is marked by GFP expression (green) and F-actin is marked by TRITC-conjugated Phalloidin (magenta). **B–** Scatterplot of the ratio between the *nub*-expressing domain (GFP) and total disc area (Phalloidin) for each condition; horizontal bars represent mean value and SD; ****-*p*<0.0001;

6. Aims

While it has been known for decades that Tropomyosins are linked to cancer states, where most studies show a causal relationship between a differential Tropomyosin expression and transformation, there is still much work to be done as to the mechanism behind Tropomyosins effect on carcinogenic transformation.

My study aims to investigate whether a Tropomyosin, *Drosophila* Tm2, affects tissue overgrowth and to uncover a possible underlying mechanism – Hippo tumor suppressor pathway.

Using *Drosophila* wing imaginal discs of 3rd instar larvae, I sought to: validate the role of Tm2 on tissue growth using independent double-strand RNA interference constructs (*tm2*-IR), targeting *tm2* to degradation (i); see if this role is isoform-specific (ii); investigate the effects of *tm2* on F-actin levels (iii); determine if Tm2 regulates Yki activity by analyzing the effect of *tm2* depletion on the expression of Yki target genes and by investigating genetic interactions between Tm2 and Hippo pathway components (iv); Finally, compare *Drosophila* and human Tropomyosin exon structures in an attempt to gain insight into any functional equivalence between them (v).

II Material and Methods

1. Fly Strains and Genetics

1.1 The Gal4-UAS system

The Gal4-UAS system is a binary transcriptional activation system native to yeast, which has been adapted to drive targeted gene expression in *Drosophila*[66]. This system consists of a transcriptional activator – Gal4 – that selectively activates any gene coding sequence (*cds*) that has been cloned downstream of an upstream activating system – UAS – sequence[67]. Gal4 does so according to the characteristics of its promotor or enhancer and thus several enhancer sequences have been "trapped" by the Gal4 gene to confer the tissue/time/position specificity of a particular enhancer[67]. As it is a binary system, the Gal4-driver component is usually physically separated from the UAS-*cds* in two distinct fly lines to avoid expression leakiness – the target gene associated with UAS is silent in the absence of its activator[66]. This allows for the easy and indefinite maintenance of both driver and reporter stocks and one driver line can be used to drive an immensity of different UAS reporter constructs widely available to the *Drosophila* community[66]. The different drivers and reporters used in this study are briefly explained in Table 1.

Table 1 | Gal4 drivers, LacZ and UAS reporters used in this study.

Gal4 driver	Spatial-temporal driver activity
nubbin-Gal4 (*nub*-Gal4)[65]	2nd instar larvae until end of larval stage; Distal wing disc (wing pouch + hinge)
hedgehog-Gal4 (*hh*-Gal4)[68]	Embryogenesis and entire larval stage; posterior compartment of embryos/wing discs
apterous-Gal4 (ap-Gal4)[56]	1st instar larvae until end of larval stage; Proximal wing disc until D-V boundary
LacZ reporter	**Operon insertion site**
ex-LacZ[69]	*expanded* gene
fj-LacZ[70]	*four jointed* gene
shg-LacZ[71]	*shotgun* (*DE-cad*) gene
UAS reporter	**Purpose**
UAS-GFP/UAS-mCherry/UAS-RFP	Highlight with fluorescent marker
UAS-*tm2*-IR^KK/UAS-*tm2*-IR^JF/UAS-*tm2*-IR^HMS	Promote *tm2* downregulation
UAS-*ex*[72]	Overexpression of *expanded*
UAS-*wts*::Myc[73]	Overexpression of *warts* tagged with Myc

1.2 Fly husbandry, maintenance and stocks

Fly stocks used in this study were maintained at RT (22-23ºC), according to standard conditions[74]. Fly line crosses were performed at 25ºC in small vials containing a yeast-glucose-agar medium with six female (F) and three male (M) flies (2:1 F/M ratio). All fly lines used in this study are in Table S1.

1.3 Crosses and stock generation

Several crosses were performed to answer specific questions.

To analyze the effect of downregulating *tm2* in the distal wing disc had on wing pouch and adult wing size, the following crosses were performed:

- [w^- ; *nub*-Gal4 ; UAS-GFP] **X** [w^- ; ;]
- [w^- ; *nub*-Gal4 ; UAS-GFP] **X** [w^- ; UAS-*tm2*-IR^{KK}]
- [w^- ; *nub*-Gal4 ; UAS-GFP] **X** [$y^- v^-$; ; UAS-*tm2*-IR^{JF}]
- [w^- ; *nub*-Gal4 ; UAS-GFP] **X** [$y^- v^-$; ; UAS-*tm2*-IR^{HMS}]

To analyze the effect of systemic *tm2* downregulation, the following crosses were performed:

- [w^- ; ; *tub*-Gal4/TM6B] **X** [w^- ; UAS-*tm2*-IR^{KK}]
- [w^- ; ; *tub*-Gal4/TM6B] **X** [$y^- v^-$; ; UAS-*tm2*-IR^{JF}]
- [w^- ; ; *tub*-Gal4/TM6B] **X** [$y^- v^-$; ; UAS-*tm2*-IR^{HMS}]

To investigate if *tm2* downregulation had an effect on Yki transcriptional targets, the following crosses were performed:

- [w^- ; *ap*-Gal4, *ex*-LacZ/CyO] **X** [$y^- v^-$; ; UAS-*tm2*-IR^{JF}]
- [w^- ; *ex*-LacZ/CyO, *wg*-LacZ ; *hh*-Gal4, UAS-GFP/TM6B] **X** [$y^- v^-$; ; UAS-*tm2*-IR^{JF}]
- [w^- ; *fj*-LacZ/CyO, *wg*-LacZ ; *hh*-Gal4, UAS-GFP/TM6B] **X** [$y^- v^-$; ; UAS-*tm2*-IR^{JF}]
- [w^- ; *shg*-LacZ/CyO, *wg*-LacZ ; *hh*-Gal4, UAS-GFP/TM6B] **X** [$y^- v^-$; ; UAS-*tm2*-IR^{JF}]

To examine the effect *tm2* downregulation on F-actin levels, the following cross was performed:

- [w^- ; ; *hh*-Gal4, UAS-GFP/TM6B] **X** [$y^- v^-$; ; UAS-*tm2*-IR^{JF}]

To study the genetic interaction between *tm2* and upstream regulators of Yki transcriptional activity, the following crosses were performed:

- [w^- ; *nub*-Gal4, UAS-*ex*] **X** [$y^- v^-$; ; UAS-*tm2*-IR^{JF}]
- [w^- ; *nub*-Gal4, UAS-*ex*] **X** [w^- ; UAS-mCherry]
- [w^- ; *nub*-Gal4, UAS-*ex*] **X** [w^- ; UAS-RFP/CyO ; UAS-*tm2*-IR^{JF}/TM6B]
- [w^- ; *nub*-Gal4,UAS-*wts*::Myc/CyO] **X** [$y^- v^-$; ; UAS-*tm2*-IR^{JF}]
- [w^- ; *nub*-Gal4,UAS-*wts*::Myc/CyO] **X** [w^- ; UAS-mCherry]

In order to measure the fluorescent area of the distal wing disc domain where both *ex* and *tm2*-IR^{JF} are ectopically expressed, the [*w*⁻ ; UAS-RFP/CyO ; UAS-*tm2*-IR^{JF}/TM6B] stock was generated (Fig.8). First, [*w*⁻ ; IF/CyO ; MKRS/TM6B] flies were crossed with [*y*⁻ *v*⁻ ; ; UAS-*tm2*-IR^{JF01095}] flies (Fig.8 green box). Resulting F1 [*w*⁻ ; IF/+ ; UAS-*tm2*-IR^{JF01095}/TM6B] and [*w*⁻ ; +/CyO ; UAS-*tm2*-IR^{JF01095}/TM6B] progeny were crossed (Fig.8 blue box) to establish the [*w*⁻ ; IF/CyO ; UAS-*tm2*-IR^{JF}/TM6B] stock (Fig.8 red box). Finally, [*w*⁻ ; IF/CyO ; UAS-*tm2*-IR^{JF}/TM6B] flies were crossed with [*w*⁻ ; UAS-RFP/CyO ; MKRS/TM6B] (Fig.8 yellow box) and the resulting F1 [*w*⁻ ; UAS-RFP/CyO ; UAS-*tm2*-IR^{JF}/TM6B] progeny was used to establish a stock (Fig.8 orange box).
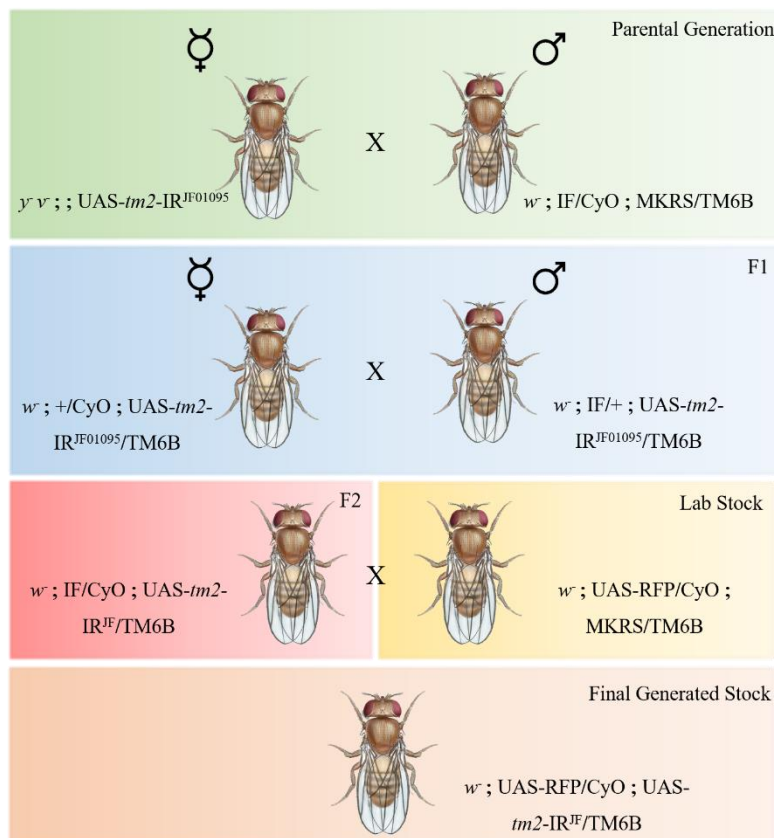
Figure 8 | Cross schematic for stock establishment

2. Immunohistochemistry

Third instar larvae were dissected in phosphate buffer solution and fixed in 4% formaldehyde in PEM (0.1M PIPES pH7,0; 2mM MgSO$_4$; 1mM EGTA) solution for 30 minutes on ice followed by a 15-minute wash in phosphate buffer + 0,2% Triton X-100 (PBT) on ice. From this point, dissected larvae were maintained in the dark. Larval remains were then left to incubate with primary antibodies in PBT and 10% donkey serum O/N at 4ºC. The following day larval remains were washed in PBT (three times, 10 minutes each) and incubated with secondary antibodies in PBT and 10% donkey serum for two hours at 4ºC. Afterwards, imaginal discs were extracted from remains and mounted between slide and coverslip in 80% Glycerol.

Primary antibodies: mouse α-Wg (1:10, 4D4 DSHB), mouse α-β-Galactosidase (1:200, Z378B Promega), rabbit α-β-Galactosidase (1:1000, 55976, Cappel).

Secondary antibodies: α-mouse (TRITC, 1:200, Jackson Immunoresearch; Alexa 647, 1:1000), α-rabbit (FITC, 1:200, Jackson Immunoresearch).

For fluorophore-conjugated Phalloidin staining, the above protocol was followed until fixation. Then, larval remains were incubated with either TRITC-Phalloidin (1:200, Sigma) or FITC-Phalloidin (1:50, Sigma) in PBT and 10% donkey serum for two hours at 4ºC. After washing in PBT (three times for 10 minutes each) wing discs were mounted in 80% Glycerol. When Phalloidin staining was coupled to immunohistochemistry, fluorophore-conjugated Phalloidin was incubated with the secondary antibodies.

3. Image Acquisition and Analysis

Confocal Z-series fluorescent images of wing imaginal discs were acquired using a confocal microscope (Leica SP5 confocal and Zeiss LSM 510 META) and low-magnification images of adult wings were acquired using a stereoscope (Leica Stereo LUMAR). Images were processed using FIJI (NIH) software and Imaris 6.4 (Bitplane) software. Standard Z-projections and cross-sections were selected and brightness and contrast was adjusted to enhance visual acuity of fluorescence.

4. Quantification and Statistical Analysis

Grayscale stereoscope images of isolated wings were processed in FIJI (NIH), where contrast was enhanced and threshold was adjusted to accurately define the contour of adult wings. The wing hinge was excluded from all measurements. The area of the wing contour was obtained using the Measure feature.

For area measurements of 3rd instar wing imaginal discs, projections of confocal Z-series, multichannel fluorescent images were also processed in FIJI.

For each channel, contrast was enhanced and threshold was adjusted to accurately define the contour of the whole wing disc (Outlined with TRITC- or FITC-conjugated Phalloidin) or of the wing pouch (*nubbin* domain marked by GFP/RFP/mCherry fluorescence). The area of the contours was obtained using the measure feature and the ratio between them was calculated as the quotient of the area of the wing pouch and the area of the whole wing disc (wing pouch/total wing disc area).

Unpaired Mann-Whitney test (nonparametric) was used to determine the statistical significance of pairwise differences in adult wing area measurements as well as differences in the ratios between wing pouch areas and total wing disc areas of wing imaginal discs. Statistical analysis and graph production was accomplished using GraphPad Prism 6 software.

5. Tropomyosin Peptide Sequence Alignment and Analysis

Coding-exon amino acid sequences for all splice variants of *tm1*, *tm2*, TPM1, TPM2, TPM3 and TPM4 were obtained from Flybase (*tm1* and *tm2*) or from GenBank (NCBI NIH) and aligned using Protein BLAST. All exons from all TPMs were aligned against each individual *tm* exon. Exons were considered similar if their alignment had a max score of 20 or greater and over 50% identity. However, exons with a max score of at least 15 and at least 35% were also taken into account, though they were considered marginally similar.

III Results

1. Two RNAi Fly Lines Target Distinct *tropomyosin2* Isoform Subsets

Preliminary results from our laboratory suggest *tm2* has a role in limiting tissue growth in *Drosophila* wing discs. As such, I am interested in validating the growth-limiting effect of downregulating *tm2* in wing discs and investigating if this effect could stem from the interaction of Tm2 with Hippo pathway signaling activity.

In order to do this, three fly lines carrying independent RNAi constructs under the control of UAS binding sites that target *tm2* to degradation were used: VDRC dsRNAi KK111307 and TRiP dsRNAi JF01095 and shRNAi HMS02260. The KK111307 and JF01095 constructs target the coding region of an exon present in all 6 isoforms (Fig.9a). The HMS02260 shRNAi targets a subset of *tm2* splice variants, allowing for greater isoform discrimination (Fig.9a).

Six splice variants have been predicted for *tm2* (Fig.9a) which generate two different isoforms. Splice variants *tm2-A/B/E/F/G* generate isoform Tm2-A/B while *tm2-C* generates isoform Tm2-C (Fig.9b). From this point onwards, the *tm2*-IR^{JF01095} and the *tm2*-IR^{HMS02260} lines will be referred to as *tm2*-IR^{JF} and *tm2*-IR^{HMS}, respectively.
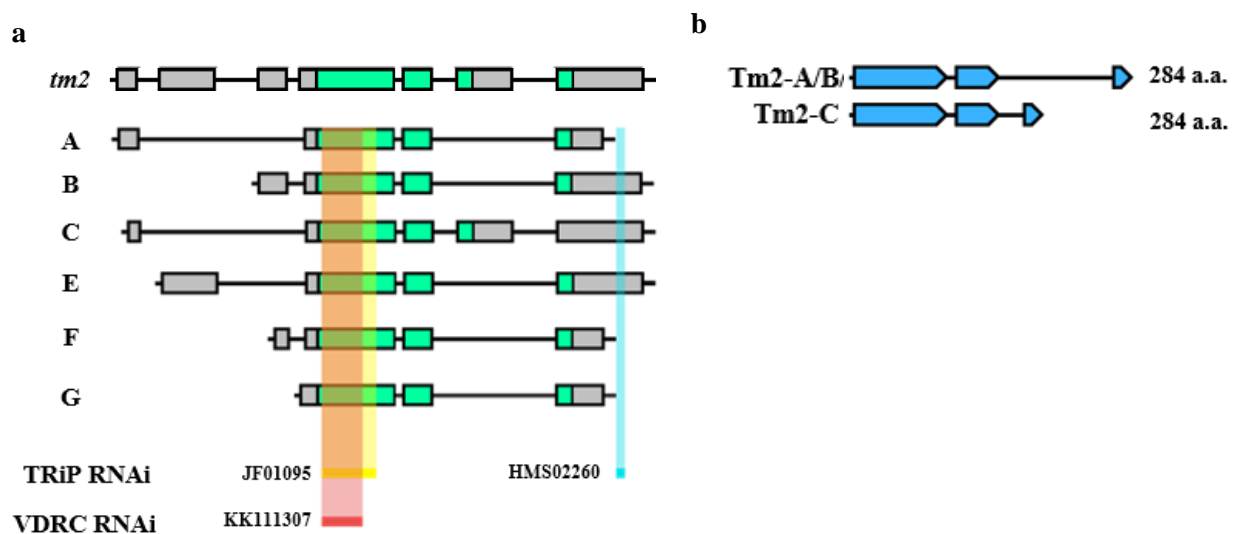
Figure 9 | *Drosophila tm2* isoforms are differentially targeted by three RNAi constructs
 a –*tm2* exon composition and domains targeted by RNAi constructs; *tm2* isoforms (A, B, C, E, F and G); coding (green boxes) and non-coding (grey boxes) regions; represent non-coding regions; shaded colored boxes represent target location of VDRC KK111307 (red), TRiP JF01095 (yellow) and HMS02260 (cyan) RNAi. **b** – *tm2* transcripts for all isoforms. a.a - amino acid.

2. *tropomyosin2* Limits Wing Overgrowth

Having verified that each fly line carries the UAS-*tm2*-IR[JF] and UAS-*tm2*-IR[HMS] transgene (S1.1 and 2.1), respectively, I next tested if driving their expression also induced overgrowth of the wing imaginal disc, as previously observed using the UAS-*tm2*-IR[KK] line (Fig.7). To do so, I have analyzed the impact of knocking down *tm2* on both the size and morphology of the adult and larval wing tissues.

2.1 *tropomyosin2* prevents tissue overgrowth in the larval wing disc

To assess the effect of *tm2* knockdown on the size of the wing imaginal discs, flies carrying either of the UAS-*tm2*-IR transgenes were crossed with flies carrying the *nubbin*-Gal4 *(nub*-Gal4) driver, which drives gene expression in the distal wing disc epithelium[65], in addition to UAS-*GFP*. Wing imaginal discs from the progeny were stained with Phalloidin, to mark F-actin. The size of the distal wing disc expressing UAS-*tm2*-IR and UAS-GFP was then evaluated. As a control, I analyzed the progeny from flies carrying *nub*-Gal4 and UAS-*GFP* crossed with *white (w-)* flies.

Wing discs expressing *tm2*-IR[HMS] (Fig.10b) showed no significant difference in size of the distal wing disc size compared to control wing discs (Fig.10a,d). However, driving *tm2*-IR[JF] in the distal wing disc (Fig.10c) led to a significant increase in the size of the GFP-expressing domain compared to both control and *tm2*-IR[HMS] wing discs (Fig.10a-d). These discs displayed a range of phenotypical penetrance. In some cases, wing discs presented an enlarged wing pouch where the typical epithelial morphology was not affected by tissue folding (Fig.10e-g). In other discs, the structural integrity of the distal wing disc was compromised, where the morphology of the wing disc was affected and overgrown tissue formed folds (fig10h-j). Thus, knocking down *tm2* using two independent RNAi (*tm2*-IR[JF] and *tm2*-IR[KK]) induces overgrowth of the distal wing disc epithelium, suggesting that *tm2* restricts growth of this domain.
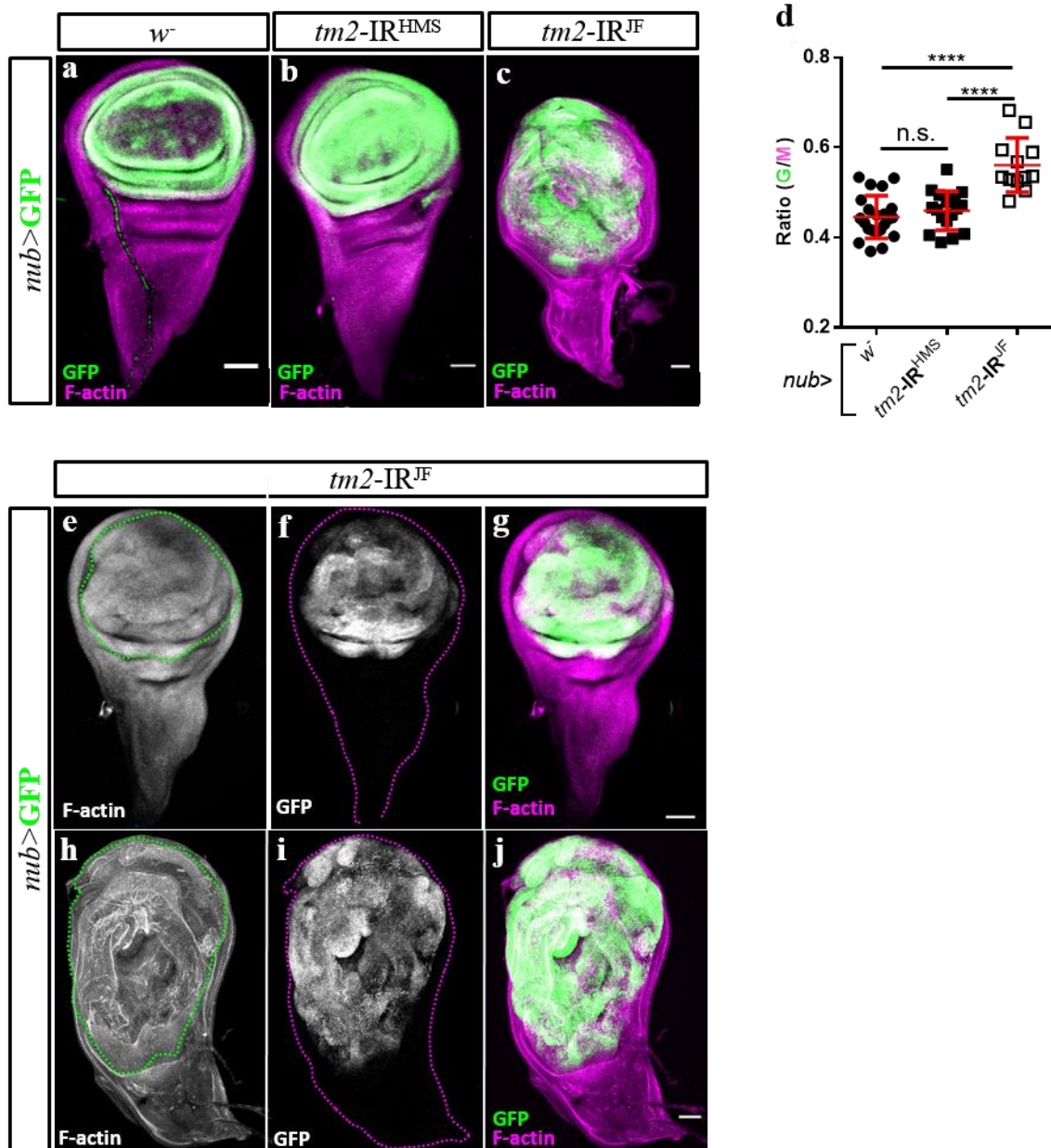
Figure 10 | Depleting *tm2* in *Drosophila* wing imaginal discs causes tissue overgrowth

a-c and **e-j** – Standard confocal projections of wing imaginal discs from 3rd instar *Drosophila* larvae where *nub*-Gal4 is driving UAS-GFP (**a**), UAS-GFP and UAS-*tm2*-IR^HMS (**b**), UAS-GFP and UAS-*tm2*-IR^JF (**c, e-j**); *nub*-expressing domain is marked by GFP expression (**f, i** - white; **a-c, g, j** - green) and F-actin is marked by TRITC-conjugated Phalloidin (**e, h** – white; **a-c, g, j** - magenta); green dotted lines outline the GFP⁺ domain; magenta dotted lines outline the total disc area, seen by Phalloidin staining. Scale bar=50µm (**a-c**) or 40µm (**e-j**). **d** – Scatterplot of the ratio between the *nub*-expressing domain (GFP) and total disc area (Phalloidin) for each genotype: *w⁻* (● n=22), *tm2*-IR^HMS (■ n=17) and *tm2*-IR^JF (□ n=12); horizontal bars represent mean value and SD; ****-*p*<0.0001; n.s – no significance.

2.2 tropomyosin2 restricts the size of adult wings

To determine if the overgrowth of wing discs knocked down for *tm2* can also be observed at adult stage, I analyzed the size of adult wings in flies expressing either of the UAS-*tm2*-IR transgenes, together with UAS-GFP, under *nub*-Gal4 control. As in the previous section, these adult wings were compared to those of control adult wing expressing only UAS-GFP under *nub*-Gal4 control. Consistent with the observations I have reported in the wing imaginal disc (Fig.10), expressing *tm2*-IR[HMS02260] did not affect the size of the adult wing (Fig.11d,g), when compared to control wings (Fig.11a), while expressing *tm2*-IR[JF] led to visibly and significantly larger wings compared to both control and *tm2*-IR[HMS] wings (Fig.11a-g).

From the results above, *tm2*-IR[HMS] seems to have no effect on wing growth, though it might have an effect if expressed ubiquitously under the control of *α-tubulin,* which encodes for a Tubulin that constitutes microtubules essential in processes such as mitosis[75]. In that sense, the different *tm2*-IR lines were driven by a *tubulin*-Gal4 (*tub*-Gal4) driver balanced with TM6B in the 3rd chromosome. The presence of TM6B balancer is phenotypically characterized by shorter and fatter larvae (*Tb*). Thus, larvae that did not have the *tub*-Gal4 driver did not express the UAS-*tm2*-IR construct and were *Tb*. If systemic expression of a given *tm2*-IR is deleterious in embryonic or early larval stages, only *Tb* larvae should be visible upon 3rd instar stage. Otherwise, both non-*Tb* and *Tb* larvae should be visible. Expressing UAS-*tm2*-IR[KK] and UAS-*tm2*-IR[JF] under the control of *tub*-Gal4 proved to be lethal, as all 3rd instar larvae were not *Tb* (Fig.11h). However, expressing UAS-*tm2*-IR[HMS] under the control of *tub*-Gal4 had no effect on the survival of larvae as both non-*Tb* and *Tb* larvae reached 3rd instar stage (Fig.11h).

These results seem to suggest that not all *tm2* isoforms contribute in regulating adult wing size and that constitutively depleting isoform Tm2-C appears to have no observable effect on survival. Together, these observations support a role for *tm2* in restricting tissue overgrowth. Since *tm2*-IR[HMS02260] had no effect on tissue size, all further analyses of *tm2* function will rely solely on *tm2*-IR[JF] for knockdown.
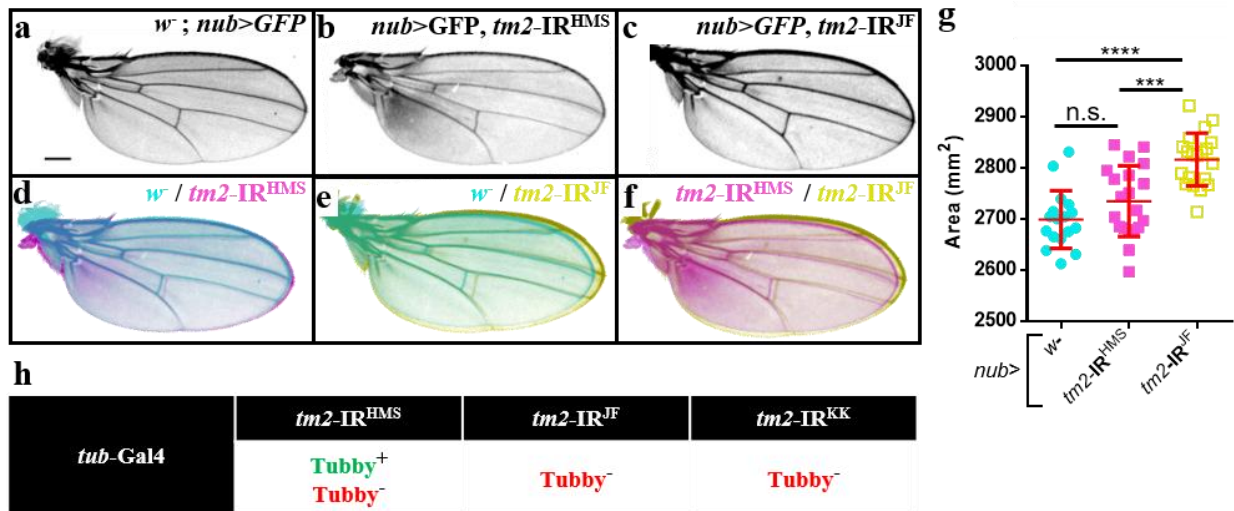
Figure 11 | Depleting *tm2* in *Drosophila* wing imaginal discs increases adult wing size

a-c – Adult wings from female flies where *nub*-Gal4 is driving UAS-GFP (**b**), UAS-GFP and UAS-*tm2*-IR[HMS] (**c**), UAS-GFP and UAS-*tm2*-IR[JF] (**d**). **d-f** – Overlapping wings of the different genotypes to highlight size differences: cyan - w[-]; magenta - *tm2*-IR[HMS]; yellow - *tm2*-IR[JF]; scale bar=0,5mm. **g** – Scatterplot of the wing area for each genotype: *w[-]* (lane 1, cyan, n=17), *tm2*-IR[HMS] (lane 2, magenta, n=20) and *tm2*-IR[JF] (lane 3, yellow, n=20); horizontal bars represent mean value and standard deviation (SD); ***-*p*<0.001, ****-*p*<0.0001, n.s.-no significance. **h** - Lethality of ubiquitous *tm2* knockdown with different RNAi lines; *tub*-Gal4 driving UAS-*tm2*-IR[HMS], -IR[JF] or UAS-*tm2*-IR[KK].

3. *tropomyosin2* limits the expression of Hippo pathway transcriptional targets

As seen above, expressing two independent RNAi constructs that target *tm2* to degradation has a pronounced effect on tissue growth in the *Drosophila* wing. The actin cytoskeleton is known to intervene in tissue growth, namely by regulating Hippo tumor suppressor pathway activity[53-55]. Given that Tropomyosins controls actin filament stability by interacting directly with actin filaments[10] *tm2* could limit wing disc growth by regulating Hippo pathway activity.

To investigate this possibility, I analyzed the effect of knocking down *tm2* on the expression levels of several Yorkie (Yki) transcriptional targets, that can be used as read out of Hippo pathway activity, including Wingless (Wg) protein, in addition to *LacZ* reporter transgenes inserted in the *expanded (ex) (ex-LacZ), four-jointed (fj-LacZ)* and *shotgun (shg-LacZ)* genes.

3.1 *expanded, wingless* and *four-jointed* expression increase upon *tropomyosin2* downregulation

For this analysis I used two Gal4 drivers: *hedgehog*-Gal4 (*hh*-Gal4) and *apterous*-Gal4 (*ap*-Gal4). The *hh*-Gal4 driver drives gene expression in the posterior compartment of wing imaginal discs[68] and the anterior can be used as an internal control. The *ap*-Gal4 driver drives gene expression in the dorsal wing disc, up to the dorsal-ventral (D-V) boundary[56] making the ventral compartment an internal control.

ex-LacZ and Wingless protein levels were analyzed in wing discs in which *tm2*-IR^{JF} expression was driven using the *ap*-Gal4 driver. Upon *tm2* depletion, *ex*-LacZ levels were visibly increased in the distal portion of the *ap*-expressing domain, where tissue morphology is affected (Fig.12a). Also, *tm2* depletion led to a considerable increase in Wg levels in the deformed D-V margin (Fig.12b), compared to the wild-type distal Wg pattern[76] which comprises of two ring-like domains in the hinge region (distal) and a stripe along the D-V boundary, dividing the distal wing disc. Using the *hh*-Gal4 driver to drive UAS-GFP and UAS-*tm2*-IR^{JF} expression in the posterior wing imaginal disc led to an increase in *ex*-LacZ levels compared to the anterior compartment (Fig.12d). This increase in *ex*-LacZ levels was even more noticeable in cross-sections through the wing disc epithelium, where *ex*-LacZ expression was higher in the GFP-positive posterior compartment (Fig.12g,h).

In addition to Wg and *ex*-LacZ, *fj*-LacZ also presented increased transcription levels in discs expressing UAS-*tm2-IR* and UAS-*GFP* in the posterior compartment using the *hh*-Gal4 driver (Fig.12i-k) compared to the anterior compartment. Cross-sections through the disc epithelium also showed a visible increase of *fj*-LacZ levels in the posterior compartment of *hh>tm2-IR, GFP*-expressing discs (Fig.12l,m).

Upon *tm2*-IR expression, *shg*-LacZ did not behave like the other Yki readouts observed above. While Wg, *ex*-LacZ and *fj*-LacZ had clearly increased fluorescence levels where *tm2* was depleted, *shg*-LacZ expression was not visibly affected in discs expressing *tm2-IR* and *GFP* under *hh*-Gal4 control, (Fig.12n-p) compared to control *hh>GFP* discs (Fig.S2), despite showing an enlargement of posterior compartment.

Furthermore, just as control discs which express GFP under *hh*-Gal4 control (Fig.S2), cross-sections through the disc epithelium present a reduction of *shg*-LacZ in the posterior compartment and an increase in *shg*-LacZ levels in the anterior compartment, adjacent to the A-P boundary (Fig.12q,r).

Similar to when *tm2*-IR is driven by *nub*-Gal4 (Fig.10), knocking down *tm2* using *hh*-Gal4 also induced tissue overgrowth with a variability in phenotype penetrance ranging from no observable overgrowth (Fig.12f) to mild tissue overgrowth (Fig.12k,p). However, these overgrowing tissues were never as strong as those induced when *tm2* is knocked down using *nub*-Gal4.

Taken together, these results indicate that *tm2* plays a role in limiting the expression of a subset of Yki transcriptional targets.
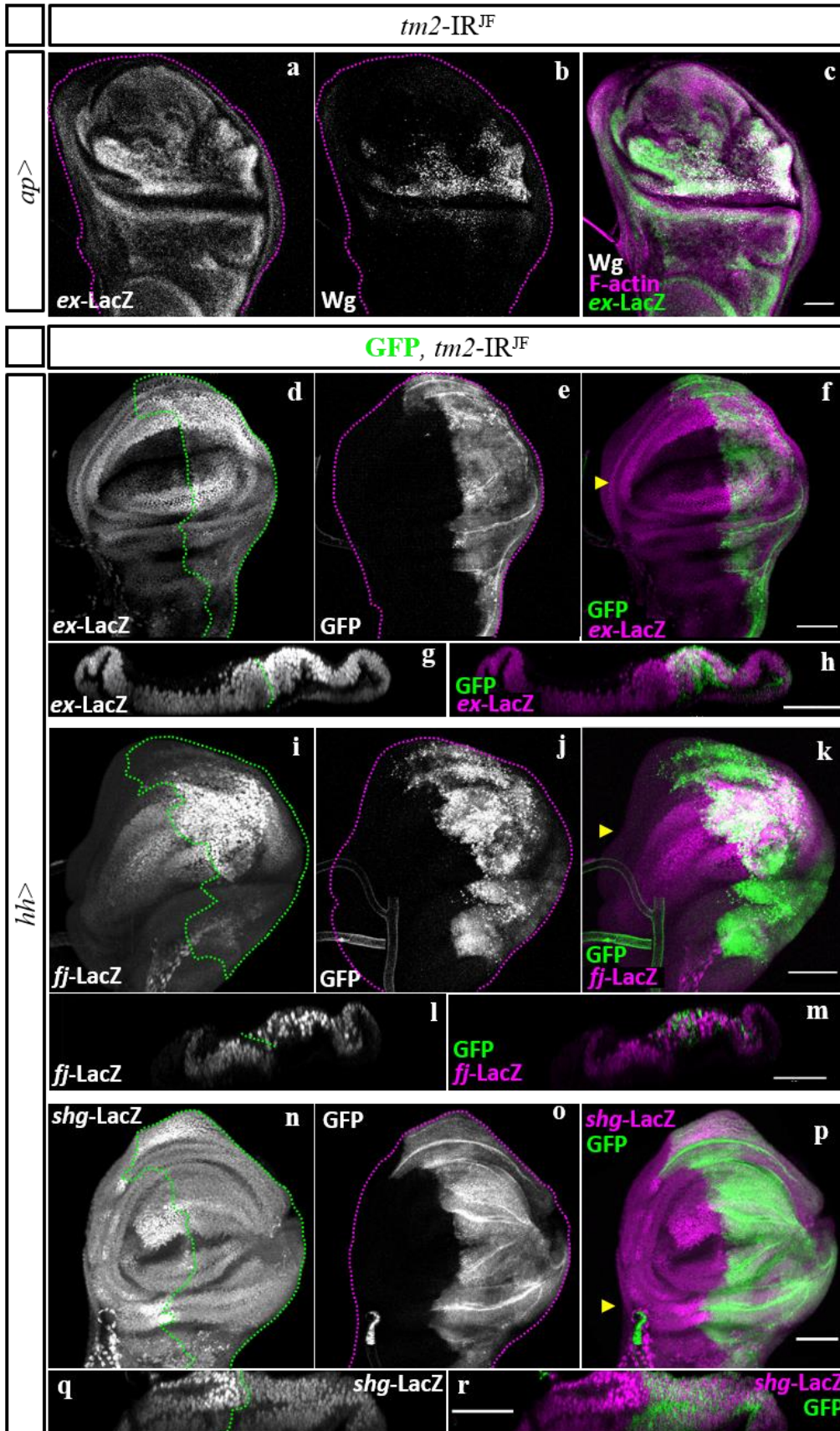
(*Figure legend on next page*)

Figure 12 | *tm2* depletion restricts the expression of a subset of Yki transcriptional targets

All panels display wing imaginal discs from 3rd instar *Drosophila* larvae**. a-r –** Standard confocal projections (**a-f, i-k, n-p**) or cross-sections through wing disc epithelia (**g, h, l, m, q, r**). **a-c –** *ap*-Gal4 driving UAS-*tm2*-IR[JF] in discs carrying *ex*-LacZ. **d-r –** *hh*-Gal4 driving UAS-*tm2*-IR[JF] in discs carrying *ex*-LacZ (**d-h**), *fj*-LacZ (**i-m**) and *shg*-LacZ (**n-r**). Posterior domain is marked by GFP expression (**e,j,o** – white; **f, h, k, m, p, r** - green); discs are stained with α-Wg (**b, c** - white), TRITC-conjugated Phalloidin (**c -** magenta) and/or α-β-Galactosidase to highlight LacZ reporters (**a, d, g, i, l, n, q –** white; **c** – green; **f, h, k, m, p, r** - magenta). Green dotted lines outline GFP-expressing domains (**d, i, n**) and separate posterior from anterior in transversal sections (**g, l, q**); magenta dotted lines outline whole disc area (**a, b, e, j, o**); yellow arrows represent cross-section position. Apical is facing up and posterior is to the right in cross-sections (**g, h, l, m, q, r**). Scale bar=50µm (**a-c**), 40µm (**d-r**).

4. Apical F-actin Accumulation is Regulated by *tropomyosin2*

The interaction between Tropomyosin and F-actin essentially underlies and brings about its function. Thus, having implicated *tm2* in the regulation of tissue growth, as well as in the expression of Yki target genes, the effect of *tm2* depletion on F-actin networks needs to be examined carefully.

To do this, I expressed *tm2-IR* and GFP in the posterior compartment of the wing imaginal disc using *hh*-Gal4 and stained these discs with Phalloidin, which marks F-actin. As previously observed, the effects of *tm2* depletion on the overgrowth of the posterior compartment showed differences in phenotypical penetrance (Fig.12). In wing discs that did not display any significant overgrowth (Fig.13a-c), there was a clear reduction of F-actin in the GFP-positive posterior compartment, compared to the GFP-negative anterior domain (Fig.13a). This reduction was more evident in cross-sections through the wing disc epithelium (Fig.13d,e). However, *hh>tm2-IR*-expressing discs that showed overgrowth of the posterior compartment, most strikingly observed in the posterior hinge domain (Fig.13f-h) accumulated F-actin (Fig.13f). This accumulation is even more striking by projecting the confocal image sections that encompass the most apical domain of the wing disc epithelium (Fig.13f'-h'). Cross-sections through the wing disc epithelium from the most ventral domain to the more dorsal domain showed that F-actin not only accumulated at the apical surface of the posterior wing disc epithelium (Fig.13i-m, yellow arrows) compared to the anterior domain separated by the A-P boundary (Fig.13i-m, green dotted line) but also more basally, characterized by abnormal dot-like F-actin structures, (Fig.13j-m).

tm2-IR^{JF}
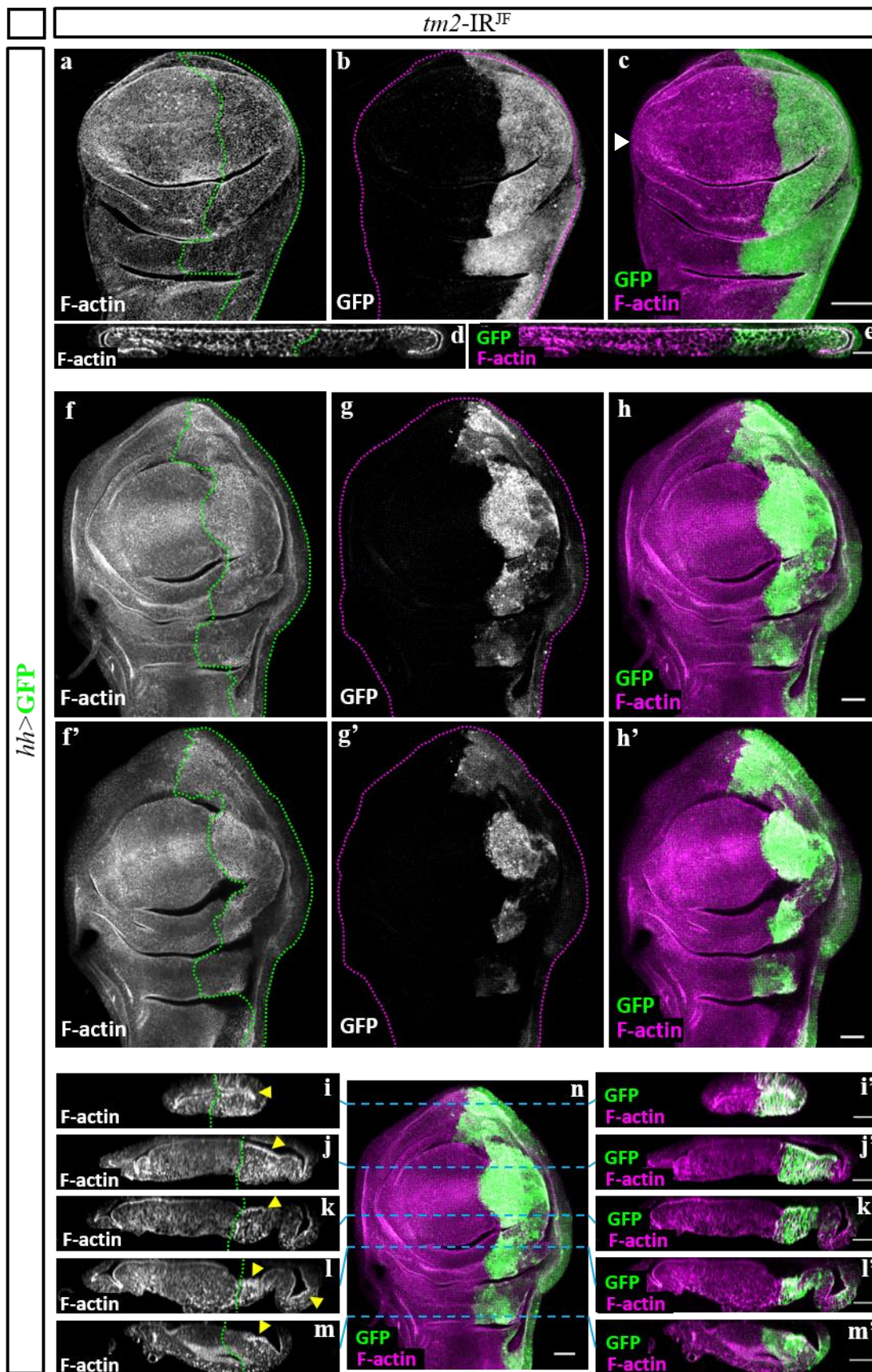
(*Figure legend on next page*)

Figure 13 | Apical F-actin accumulation is affected upon *tm2* depletion

All panels are wing imaginal discs from 3rd instar *Drosophila* larvae. **a-n –** Standard confocal projections (**a-c, f-h, f'-h', n**) or cross-sections through the wing disc epithelium (**d, e, i-m, i'm'**) in which *hh*-Gal4 is driving UAS-GFP and UAS-*tm2*-IR^JF. Posterior domains are marked by GFP expression (**d, b, g, g'** - white; **c, e, h, h'-m', n** - green); discs are stained with TRITC-conjugated Phalloidin (**a, d, f, f', i-m** - white; **c, e, h, h', i'-m', n** - magenta). **f'-h' –** projection of the epithelium apical domain of the same disc. Green dotted lines outline GFP-expressing domains (**a, f, f'**) or the anterior-posterior boundary (**i-m**); magenta dotted lines outline the whole disc area; white arrow (**c**) and blue dotted lines (**n**) indicate the position of each cross-section; yellow arrows indicate apical F-actin accumulation. Apical is facing up and posterior is to the right in cross-sections (**d, e, i-m, i'-m'**). Scale bar=50µm (**a-c**), 20µm (**d-n, f'-m'**).

5. *tropomyosin2* Interacts with *warts*, an Upstream Regulator of Yorkie Activity

Considering the above results, *tm2* seems to play a role in limiting the expression of Yki transcriptional targets as well as in preventing apical F-actin accumulation. These two effects could very well be linked through Hippo pathway activity; as apical F-actin levels have been shown to be regulated by Hpo kinase cascade activity. As such, the effect *tm2* has on F-actin accumulation and growth could be by interacting with Hippo pathway components. In an attempt to determine the level at which *tm2* might contribute in regulating Hippo pathway activity, *tm2* was depleted alongside the overexpression of two upstream regulators of Yki – *wts* and *ex*. This was done to see whether *tm2*-IR expression could rescue the growth-suppression phenotype of *wts* and *ex* overexpression. Both adult wings from female flies and wing imaginal discs from 3rd instar larvae were used for this analysis.

5.1 *tropomyosin2* interacts with *warts*, but not *expanded* in regulating adult wing size

In this experiment, I express UAS-*tm2*-IR^JF together with either UAS-*ex* or UAS-*wts* transgenes using a *nub*-Gal4 driver to observe if *tm2* downregulation rescues *ex*- or *wts*-induced undergrowth. As a control for *tm2* depletion, either UAS-*ex* or UAS-*wts* transgenes along with a UAS-mCherry transgene are driven by *nub*-Gal4 in order to have the same number of UAS-transgenes in both conditions. As a control for the effect of *ex* or *wts* overexpression, wild-type (*w*⁻ background) individuals with a UAS-GFP transgene are driven by nub-Gal4.

As expected, when overexpressing either *ex* (Fig.14b) or *wts* (Fig.14c) with the *nub*-Gal4 driver, adult wings were significantly smaller than wings where UAS-GFP was expressed in a *w*⁻ background (Fig.14a,j). *wts* was more potent in reducing wing size than *ex*, as *wts*-overexpressing wings were significantly smaller (Fig.14j).

In contrast and as previously observed (Fig.11), expressing *tm2*-IR^{JF} with UAS-GFP significantly increased wing size compared to when UAS-GFP was expressed in a *w*$^-$ background (Fig.11e,g). However, expressing *tm2*-IR^{JF} did not affect the size of *ex*-overexpressing wings, as wing size was not significantly different to those of *ex*- and mCherry-expressing adult wings (Fig.14h,j). Surprisingly, *tm2*-IR^{JF} expression significantly aggravated growth suppression induced by *wts* overexpression (Fig.14i,j). The fact *tm2*-IR^{JF} has no effect on *ex*-induced growth suppression could possibly indicate *tm2* might interact with Hippo pathway upstream of Ex while the effect *tm2*-IR^{JF} expression has on *wts*-induced growth suppression contradicts what I have shown so far of the growth-restricting effect of *tm2*. However, wings where *wts* and *tm2*-IR^{FJ} were ectopically expressed presented a heavily affected morphology, with folded and irregular wing-edges as well as fused wing veins (Fig.14f). As such, adult wing size might not be the ideal readout for the interaction between *ex* or *wts* and *tm2*.
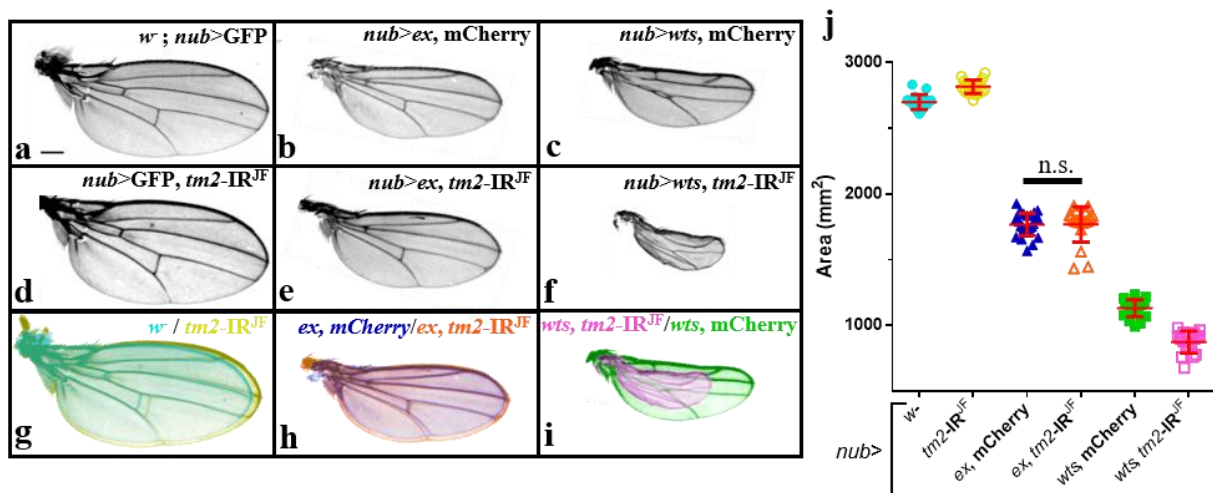
Figure 14 | Depleting *tm2* in *wts*-overexpressing wings heavily affects wing morphology and size
a-f – Adult wings from female flies in which *nub*-Gal4 is driving UAS-GFP (**a**), UAS-*ex* and UAS-mCherry (**b**), UAS-*wts* and UAS- mCherry (**c**), UAS-GFP and UAS-*tm2*-IR^{JF01095} (**d**), UAS-*ex* and UAS- UAS-*tm2*-IR^{JF01095} (**e**), UAS-*wts* and UAS- UAS-*tm2*-IR^{JF01095} (**f**). **g-i** – Overlapping wings of the different genotypes to highlight size differences: cyan - *w*$^-$; yellow - *tm2*-IR^{JF}; blue - *ex*, mCherry; orange - *ex*, *tm2*-IR^{JF}; green - *wts*, mCherry; magenta - *wts*, *tm2*-IR^{JF} ; scale bar=0,5mm. **j** - **h** – Scatterplot of the wing area for each genotype: *w*$^-$ (lane 1, cyan, n=17), *tm2*-IR^{JF} (lane 2, yellow, n=20), *ex*, mCherry (lane 3, blue, n=27); *ex*, *tm2*-IR^{JF} (lane 4, orange, n=20); *wts*, mCherry (lane 5, green, n=21); *wts*, *tm2*-IR^{JF} (lane 6, magenta, n=18); horizontal bars represent mean value and SD; all statistical differences between conditions are significant with $p<0.0001$ unless indicated otherwise; n.s.-no significance.

5.2 *tropomyosin2* does not interact with *expanded* in regulating wing imaginal disc size

I next looked at the interaction of *tm2* and *ex* in wing discs in order to confirm results from adult wings and avoid possible problems they encounter in analyzing the effect gene interaction has on tissue size. In agreement with my previous observations showing that overexpressing *ex* reduces the growth of the adult wing (Fig14), overexpressing *ex* with *nub*-Gal4 significantly reduced the size of the distal wing domain relative to the size of the whole wing disc (Fig.15a,c,e). However, and still in agreement with results from adult wings, *tm2* depletion combined with *ex* overexpression had no observable effect on the ratio between *nub* domain area and total disc area (Fig.15c,d,e).

tm2 thus seems to interact with *wts*, though in an unexpected manner contrary to the role of *tm2* as a growth suppressor. However, the interaction between the two could be unrelated with Hippo pathway activity. While *tm2* appears not to interact with *ex*, this might simply mean it feeds into Hippo pathway upstream of Ex.
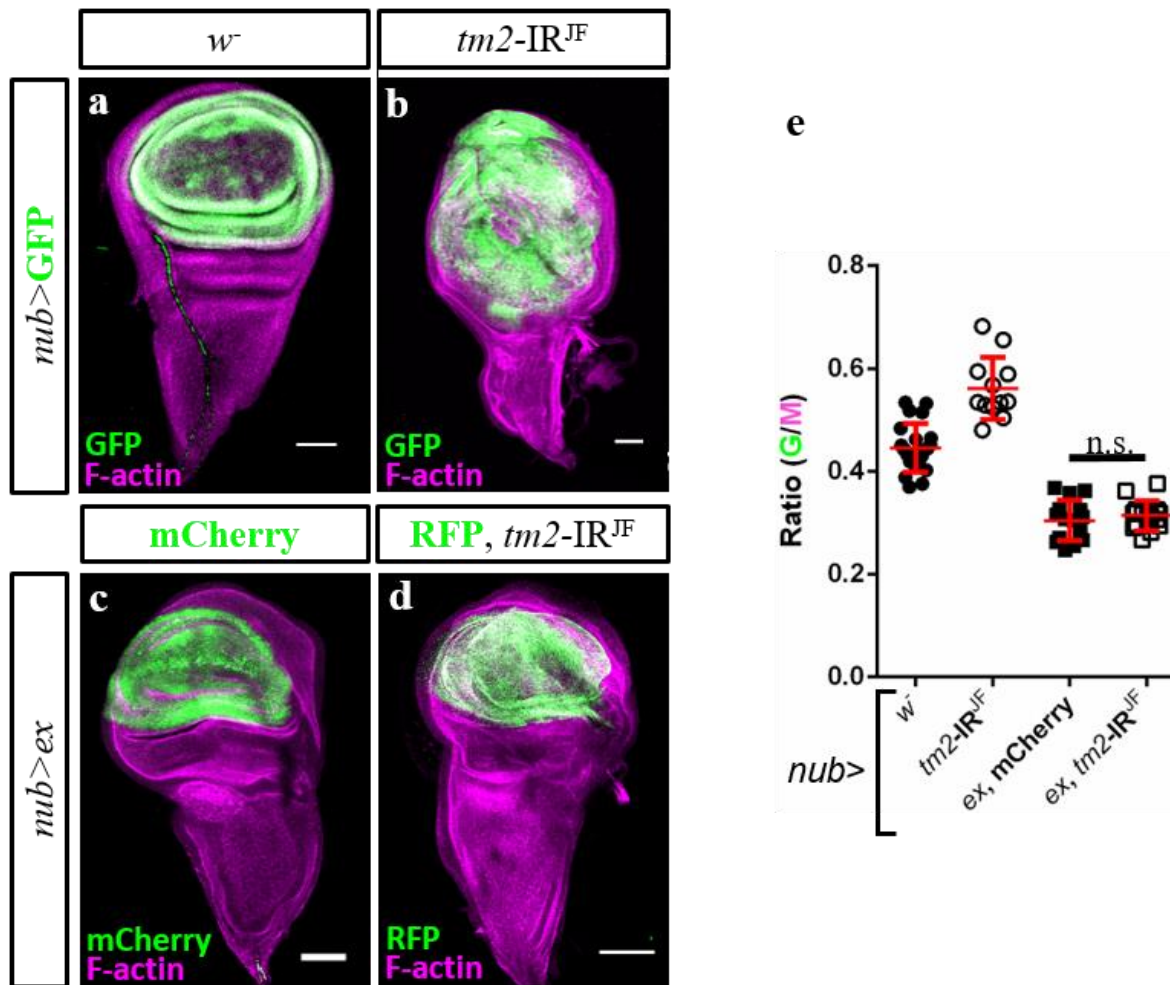
Figure 15 | Depleting *tm2* has no effect on *ex*-induced growth suppression in the wing pouch

a-d – Standard confocal projections of wing imaginal discs from 3rd instar *Drosophila* larvae in which *nub*-Gal4 is driving UAS-GFP (**a**), UAS-GFP and UAS-*tm2*-IRJF01095 (**b**), UAS-*ex* and UAS-mCherry (**c**), UAS-*ex* and UAS-RFP and UAS-*tm2*-IRJF01095 (**d**); The *nub*-expressing domain is marked by GFP (**a, b**- green) or mCherry (c - green) or RFP (d - green). Discs are stained with TRITC-conjugated (**a, b** - magenta) or FITC-conjugated Phalloidin (**c, d** – magenta) to mark F-actin; Scale bar=50µm. **d** – Scatterplot of the ratio between *nub*-expressing domain and the total wing disc areas for each genotype: *w*⁻ (● n=22), *tm2*-IRJF (○ n=12), *ex* and mCherry (■ n=15) and *ex* and *tm2*-IRJF (□ n=14); horizontal bars represent mean value and SD; all statistical differences between conditions are significant (p<0.0001) unless indicated otherwise; n.s.-no significance.

IV Discussion

HMW Tropomyosins have a tumor-suppressor function *in vitro*, discovered using human cell lines[40]. However, this function has not yet been validated *in vivo*. Given the conserved nature of Tropomyosins throughout Metazoans[17] and the similarities in exon composition between *tm2* and TPMs, I investigated whether *tm2* has a tumor-suppressor role in the *in vivo* model *Drosophila melanogaster*. My observations suggest that the Tm2-A/B isoform is required to prevent wing disc overgrowth in the later stages of development by regulating Hippo pathway activity. These findings suggest a possible mechanism by which other Tropomyosin isoforms exert their tumor-suppressor activity.

Hence, I propose that a Tm2-A/B decorated F-actin network is essential in translating compressive forces generated in growing discs into Hippo pathway activation and growth termination.

1. Tm2-A/B May be Responsible for Restricting Wing Disc Growth

My results suggest that Tm2-A/B, but not Tm2-C is required to maintain normal tissue size by restricting tissue overgrowth in imaginal wing discs. Downregulation of all *tm2* splice-variants using two different RNAi transgenes – *tm2*-IR[JF] and *tm2*-IR[KK] – led to tissue overgrowth. The *tm2*-IR[JF] line was used in addition to the KK line, because flies from this collection may have an unintended secondary insertion site for the RNA hairpin vector in the 5' UTR of *tio*[77,78]. Different KK RNAi lines led to recurrent phenotypes unrelated with the targeted genes, such as wing inflation problems, Yki-induced tissue overgrowth and pupal lethality[78], thereby affecting these line's reliability.

The additional RNAi line would also prove useful in ruling out the possibility of an off-target effect. Unfortunately, both *tm2*-IR[KK] and *tm2*-IR[JF] have a 19bp off-target region for DMAP1, a DNA methyltransferase-associated protein that interacts with the NF-κB transcription factor in modulating innate immune response[79].

By using the *tm2*-IR[JF] line from the TRiP, I was able to assure the overgrowth phenotype was not due to a faulty insertion site in the *tm2*-IR[KK]. Then again, since both lines have the off-target region for DMAP1, I cannot discard the possibility that the overgrowth phenotype of wing discs expressing either RNAi is due to DMAP1 downregulation. As such, it is still necessary to demonstrate the overgrowth of wing discs expressing *tm2*-IR[KK] and *tm2*-IR[JF] is due to *tm2* depletion and rule out the off-target as a possible cause. This can be done by driving the expression of *dmap1*-IR in the distal wing compartment and see whether wing discs present a tissue overgrowth phenotype as with the *tm2*-IR[KK] and *tm2*-IR[JF] lines.

In addition, if the overgrowth phenotype results from *tm2* depletion, expressing *tm2* along with *tm2*-IR is expected to suppress wing disc overgrowth. Finally, the effect of *tm2* on wing disc growth should be confirmed by inducing clones mutant for a *tm2* allele specific for all the splice variants. In this case, overgrown clones would be expected but only if wing discs are close to growth termination, according to the overarching hypothesis of Tm2-A/B translating compression into growth halt.

tm2-IR[JF] depletes all six *tm2* splice variants and leads to tissue overgrowth (Fig.10). In contrast, *tm2*-IR[HMS] depletes the only splice variant that codes for Tm2-C in addition to two of the five splice variants which code for Tm2-A/B and does not lead to overgrowth (Fig.10). Because the Tm2-A/B isoform is probably still expressed in *tm2*-IR[HMS]-expressing wing discs, this isoform is likely the only one restricting wing growth. In agreement with this possibility, clones mutant for the *tm2*[ZCL2456] allele, which prevent the production of the Tm2-C isoform specifically, do not overgrow when compared to their sibling twin spots (F. Janody, unpublished). Although to confirm that Tm2-A/B, but not Tm2-C, restricts wing disc growth, a clonal analysis should be done using a *tm2* allele that prevents the production of Tm2-A/B entirely, to observe if mutant clones were significantly larger than their twin-spot counterparts. This, along with a Western Blot to quantify Tm2 isoform levels, would indicate if Tm2-A/B restricts wing disc growth. Nevertheless, a growth-related phenotype is only to be expected in a later stage of wing disc development, when compression forces could lead to growth termination. As such, in some cases there might not be enough time to observe overgrowth.

Surprisingly, the overgrowth phenotype generated by depleting Tm2-A/B with *tm2*-IR[JF] was highly variable, ranging from almost wild type (Fig.10e-g) to drastically overgrown (Fig.10h-j). Even though all larvae were dissected at 3rd instar, this variability probably stems from subtle differences in developmental stage. This could indicate that Tm2-A/B is only required to halt wing disc growth when tissues have reached their final size, suggesting it either has no function in growth control before then or only starts to be expressed when wing discs are close to reaching their final size. Though to confirm these observations, I would need to properly stage *tm2*-IR[JF]-expressing larvae and determine whether there is a correlation between phenotype penetrance and developmental time.

2. Tm2-A/B and Tm2-C May Have Opposite Effects on F-actin levels

Cooperative binding to F-actin is a universal and central property of Tropomyosins, through which they exert their wide array of cellular functions[11,80]. As such, the tumor-suppressor function of Tm2-A/B is likely a consequence of regulating a particular F-actin subtype. This is consistent with how mammalian tumor-suppressing Tropomyosin isoforms function, where their tumor-suppressor activity depends on how they regulate a specific F-actin subtype or network, such as stress fibers[12,36,40]. For instance, the loss of HMW Tpm isoforms is associated to stress fiber disruption and subsequent motility increase and invasiveness of tumor cells[40].

tm2 depletion using *tm2*-IR[JF] had varying effects on growth (Fig.10). When *tm2*-IR[JF] expression appears to affect normal disc growth, it is accompanied by an increase in F-actin levels (Fig.13f-h). However, when *tm2*-IR[JF] expression had no visible impact on growth, F-actin levels decreased (Fig.13a-e). My results suggest that at early stages, Tm2-A/B has no role in controlling growth, thus the decrease in F-actin levels at early stages could be due to Tm2-C reduction. In agreement with this hypothesis, clones mutant for the *tm2[ZCL2456]* allele, which prevents the production of the Tm2-C isoform specifically, show reduced F-actin levels (F. Janody, unpublished).

Based on these findings, Tm2-C could be required for maintaining normal F-actin levels by promoting F-actin accumulation, while Tm2-A/B could maintain normal F-actin levels by preventing filament accumulation. This is not surprising given several studies that report contrasting effects on actin filament polymerization by different Tropomyosin isoforms, due to their stabilizing effect, as well as their isoform-specific effect on recruiting distinct ABP to F-actin[81-83].

Tm2-C may promote F-actin accumulation by several mechanisms. Tm2-C-covered actin filaments could compete for ADF/Cofilin binding and thus protect filaments from severing, as is the case of Tpm3.1[12,30], Tpm1.1[84,85] and yeast Cdc8[86]. Similarly, Tm2-C could also prevent Gelsolin severing, since HMW Tropomyosins seem to partially protect filaments from severing and can even anneal Gelsolin-severed F-actin[11]. Tropomodulin, which has been shown to cap filaments and prevent pointed-end elongation and depolymerization[11]. As such, Tm2-C could be required to prevent pointed-end depolymerization together with Tropomodulin. Tm2-C could also promote F-actin accumulation by mediating F-actin nucleation by Formins, as these have been proposed to act as orchestrators of the Tropomyosin composition of F-actin at the time of nucleation. Formins have been shown to recruit different Tropomyosin isoforms[30]. Finally, Tm2-C could directly stabilize F-actin, as Tpm1.1 and LMW Tropomyosin isoforms have been shown to have a stabilizing effect, which leads to longer filaments[14,87].

Tm2-A/B, however, could prevent F-actin accumulation at the end of larval wing disc development. In spite of most Tropomyosin isoforms protecting F-actin from ADF/Cofilin-mediated disassembly, some isoforms (Tpm1.7, Tpm2.1 and Tpm4.2) promote filament severing[11,88,89]. This way, Tm2-A/B may be required to prevent F-actin accumulation by promoting Cofilin-mediated filament disassembly. Tropomyosins have also been shown to inhibit Arp2/3-dependent actin nucleation[11,30]. Tm2-A/B could therefore prevent the formation of branched actin networks nucleated by Arp2/3, similarly to what has been shown for Tpm1.6, Tpm1.7 or Tpm1.1[30].

Moreover, Tropomyosins have also been shown to regulate myosin motor activity[90]. This could influence contractile properties of F-actin structures such as the actomyosin cortex[1,91] and filament turnover, as myosin-induced contraction has emerged as a mechanism of actin network disassembly[1]. In fact, the same Tropomyosin isoform can stimulate one myosin motor and inhibit another[11,30,88]. Thus, Tm2-A/B could recruit a myosin motor that maintains filament turnover, preventing F-actin accumulation or exclude a particular myosin motor which has the ability to alter the mechanical properties of the network, leading to F-actin accumulation.

While these hypotheses propose possible mechanisms by which Tm2-C and Tm2-A/B might affect F-actin accumulation, most of these hypotheses are based on interactions between Tropomyosin, F-actin and ABP, which have mostly been described *in vitro*. Therefore, more insight on the *in vivo* interaction between Tropomyosins and other ABPs is needed. While there is still a modest amount of studies that investigate *Drosophila* Tropomyosins in non-muscle cells, the subject has been garnering attention of late. This presents an opportunity to further investigate the interaction between Tropomyosin, F-actin and other ABPs, as it has been done in yeast, *C. elegans* and human cells[37,38,61,92].

3. Tm2-A/B: a Link Between Mechanical Force and Growth

The role of Tm2-A/B in preventing F-actin accumulation and in regulating wing growth are likely connected. Interestingly enough, it was in our laboratory where it was first described that the actin cytoskeleton regulates growth via interaction and regulation of the Hippo tumor suppressor pathway[56] and further studies contributed to better define this regulation[55,57,58,59]. These studies indicate that the Hippo pathway kinase cascade activity restricts F-actin accumulation (Fig.16). CP and Ex prevent apical F-actin accumulation which in turn inhibits kinase cascade activity and increases Yki transcriptional activity. Furthermore, promoting apical F-actin accumulation by preventing the capping activity of capulet (capt) or by overexpressing diaphanous (a formin) also led to decreased Hippo pathway activity[56,57]. On the other hand, Zyx appears to promote Yki activity by antagonizing Ex in regulating a different F-actin network, as this effect of Zyx on Yki activity is independent of Hippo kinase cascade activity[58]. In a similar way, a Tm2-A/B governed F-actin network, distinct from the previous one, could be required to halt tissue growth in later stages of wing disc development (Fig.16). This network would be distinct from the above due to the apparent temporal requirement in the regulation of F-actin levels and growth by Tm2-A/B. For instance, *cp* downregulation led to a consistently overgrown wing disc phenotype[56] while *tm2* downregulation appears to only have an effect on F-actin levels and growth at the end of larval wing disc development (Fig.10 and 13).
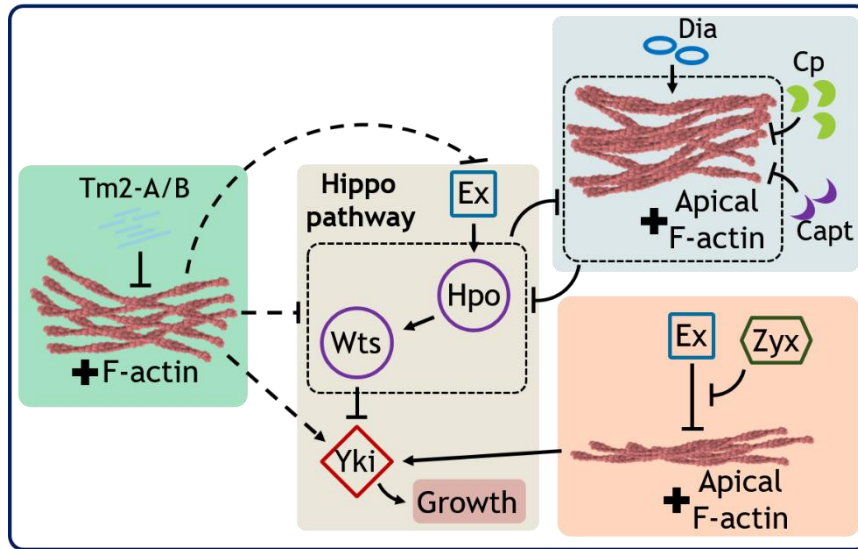
Figure 16 | Hippo pathway regulation by distinct F-actin networks

Green box - Proposed F-actin network controlled by Tm2-A/B which prevents filament accumulation and is required to limit tissue overgrowth by preventing the upregulation of Yki transcriptional targets. **Blue box -** Actin filament networks where CP and Capt prevent and Dia promotes F-actin accumulation; **Orange Box -** Zyx promotes growth by antagonizing Ex-mediated F-actin regulation. **Beige box –** Simplified Hippo pathway schematic.

To estimate the expression levels of several Yki transcriptional targets, I looked at the levels of LacZ expression in several reporter lines for Yki transcriptional targets upon *tm2*-IR[JF] expression. I was able to see an increase in LacZ reporters for *ex* and *fj*, but not *shg*. Although *shg* expression has been shown to increase upon directly inactivating *hpo*[93,94], the output of Hippo signaling is cell-type specific and the subset of Yki transcriptional targets is known to be quite variable since it depends on the binding partner of Yki[48]. However, increased *shg* expression upon hpo inactivation was seen in wing discs and *shg* regulatory region has a binding site for Sd, the main transcription factor that binds Yki to regulate transcription[93]. Despite this, there may be other players involved and other binding partners, as many are still thought to be undiscovered. Altogether, *ex* and *fj* upregulation in addition to increased Wg levels (Fig.12) suggest that Tm2-A/B is necessary to keep Yki transcriptional activity in check. While this regulation of Yki activity is most likely due to Tm2-A/B alone since Tm2-C has no effect on growth, there would need to be no visible change in the expression levels of Yki transcriptional targets in clones lacking Tm2-C as well as *tm2*-IR[HMS] expressing tissues to properly establish this.

Therefore, a F-actin based structure unlike those previously described, defined by Tm2-A/B, might be receiving external cues and translating them into Hippo pathway regulation to control Yorkie transcriptional activity in order to stop tissue growth at the end of wing disc development.

Given that actin cytoskeletal dynamics are widely regarded as the central contributors and mediators of mechanical force generation in the cell environment[1], one external cue this network could translate into Hippo pathway-mediated growth suppression is mechanical force.

Additionally, mechanical forces have been proposed to regulate the termination of growth and thus define the final dimensions of organs[95-98]. In *Drosophila* wing discs, cells in the wing pouch are compressed while cells in the periphery are stretched[95,96] and computational models backed by experimental data propose that compressive forces feed into a feedback mechanism that may regulate tissue growth, leading to growth termination[98].

While my work did not investigate the mechanical component underlying this hypothesis, a Tm2-A/B-dependent network could act as a sensor of mechanical information leading to the activation of Hippo pathway, halting wing disc growth (Fig.17). Thus, before reaching a certain developmental stage, wing discs lack sufficient compression to activate Hippo signaling in a Tm2-A/B-dependent manner. In contrast, the compressive forces in the wing pouch reach a threshold later in development, where a Tm2-A/B containing F-actin network translates mechanical force into Hippo pathway activation.
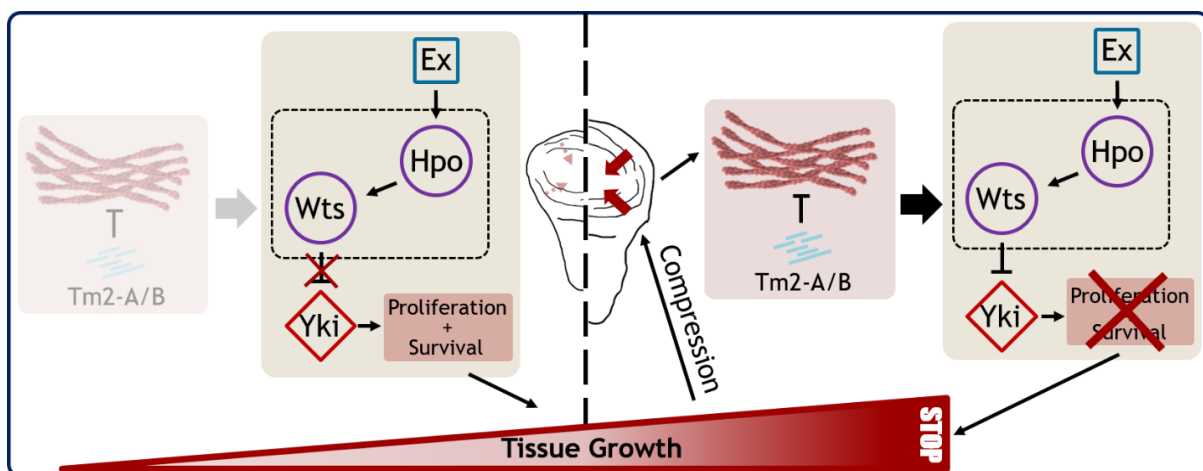
Figure 17 | Model of a Tm2-A/B-dependent F-actin network which translates force into Hippo pathway activation, halting wing disc growth in late development of wing imaginal discs

In this model, Tm2-A/B is key in translating the build-up of compressive forces in late development into growth termination. Earlier in development (left side), This network has no impact on growth and Hippo pathway is inactive, allowing tissues to grow. Later in development (right side), as tissues grow compressive forces are built up to reach a threshold. These forces, in turn, are translated to a Tm2-A/B-dependent F-actin network which activates Hippo pathway and subsequently promotes wing growth arrest.

Hippo pathway activity has been shown to respond to mechanical forces[49,53-55] in regulating Yki activity. Two particular studies link cytoskeletal tension to YAP/TAZ activity[99,100]. In these studies, increasing the stiffness of cells' environment led to YAP activity while restricting cell adhesion area or increasing cell-cell contact inhibited YAP activity. What these studies suggest is that tension leads to Yki activity while compression prevents Yki activity. Reducing the available spreading area mimics high cell-density conditions, which are prone to higher compression forces. A more recent in vivo study not only links cell density and Yki activity, but also shows F-actin is key in maintaining that link *in vivo*[101]. They report that an increase in cell density during zebrafish blastemal formation leads to inactive Yki via actin cytoskeleton regulation, as disrupting F-actin dynamics overrides high density cues and leads to Yki activity. This last study, along with others tightly link the actin cytoskeleton with mechanical force generation/transmission as well as both of these with Hippo pathway activity, which is in complete agreement with my proposed model.

I propose that Tm2-A/B is only involved in growth termination when discs have reached a certain size. If so, in undergrown discs, the function of Tm2-A/B would be dispensable. In agreement with my model, *tm2* downregulation had no impact on growth suppression caused by *ex* overexpression, both in adult and larval tissues (Fig.14 and 15).

Surprisingly, *tm2* downregulation seems to aggravate *wts*-induced growth suppression in adult wings (Fig.14). Besides controlling Yki phosphorylation, Wts regulates several cell processes such as mitotic exit, cell growth, and morphogenesis[102]. In *Drosophila*, Wts has been suggested to have diverse substrates, including Yki[103] and was shown to have a Yki-independent role in promoting growth arrest, apoptosis and autophagy in salivary glands[104] and regulating dendrite patterning and maintenance[105]. Thereby, a distinct Tm2-dependent F-actin network could be involved in limiting the ability of Wts to affect cell survival or patterning. This would explain the heavily affected morphology of wings where *wts* and *tm2*-IR[FJ] were ectopically expressed (Fig.14f). Even though I have presented evidence suggesting a Tm2-A/B-decorated F-actin network limits wing disc growth by regulating Hippo pathway activity, it is still unclear at what level in Hippo pathway this F-actin network might act. To investigate how Tm2-A/B controls Hippo pathway activity, I need to gauge Tm2-A/B loss in assays where wing discs will be in a developmental stage where Tm2-A/B will be relevant for growth. It would also be very relevant to induce compressive or distensile forces in wing discs and see whether these forces lead to changes in Hippo signaling when Tm2-A/B is absent or overexpressed. This would solidify our claim and maybe validate mechanical force as a growth-modulating signal *in vivo.*

While the model I propose for Tm2-A/B as a translator of mechanical force into Hippo pathway-mediated growth arrest is quite interesting and exciting, there are reports linking Tm2 to nuclear division and cell-cycle[21,23] that must be taken into account.

One report[21] indicates that Tm2-C, along with Tm1 and Tpn, is required in maintaining genomic stability, as embryos mutant for each of these components present abnormal nuclear divisions with spindle malformations and aneuploidy, while the other indicates Tm2-A/B and Tm1-J populate a F-actin network surrounding the Golgi apparatus, maintaining its integrity and regulating cell-cycle progression[23]. As it stands, the possibility that the role of Tm2-A/B in cell-cycle progression could contribute towards growth regulation in wing discs cannot be ruled out. However this role of Tm2 alone is unlikely to explain the overgrowth phenotype upon *tm2* downregulation, as aneuploidy by itself seems to be insufficient to drive tumorigenesis, despite being a key factor in cancer progression[106]. One way to clearly determine if Tm2-C and/or Tm2-A/B play a role in genomic stability of wing imaginal disc cells would be to observe if there is any spindle malformation or faulty chromosome segregation upon Tm2-C or Tm2-A/B depletion and if any of these isoforms are located in the nucleus.

4. *Drosophila* as a Model in the Study of Tropomyosins in Cancer

This study stems from the observation that TPM2 is downregulated in pre-malignant breast tumor samples and in an inducible human epithelial cell line which recapitulates the multistep development of cancer (Tavares *et al.,* in revision).

I found that all exons from all human Tropomyosins had similarities to exons of both *tm1* and *tm2*, with no preferential contribution of either *tm* to a particular TPM (S2.3). This is in agreement with what is known from Tropomyosin function in muscle, which has established human TPMs as orthologs of *Drosophila tms*[17,25]. *tm1* isoforms seem to be more relatable to LMW human isoforms given that the contribution of *tm1 to* LMW-exclusive and required human exon 1b is much greater than that of *tm2*, whose exon 1 has only marginal similarities with human exon 1b (Fig.S3). Moreover, *tm1* lacks any similarity to HMW-exclusive human exon 2a while exon 1 of *tm2* has some sequence similarities to exon 2a (Fig.S3). This points to the possibility of *tm2* gene products being more relatable to HMW human Tropomyosin isoforms while *tm1* splice variants could be functionally equivalent to LMW human Tropomyosin isoforms. Together with the fact that downregulating *tm1* in the preliminary screen done in our lab led to tissue undergrowth (F. Janody, unpublished), these indications agree with the protective effect HMW Tropomyosins have in tumorigenesis and with the tumor-suppressor effect Tm2-A/B suggested previously.

This analysis alone was not able to determine a clear and distinguishable contribution of *tm2* towards a particular human tropomyosin gene. It does, however, seem to argue in favor of *Drosophila* as a capable in vivo model to study human Tropomyosin function and quite possibly further investigate the mechanisms behind the role Tropomyosins have in cancer progression.

5. Final Remarks

A fundamental question of developmental biology is how growth is regulated to produce organs of different sizes. While much knowledge has been attained concerning how tissue expansion is achieved, the mechanism by which tissues stop growing remains unclear. In this sense, Tm2-A/B might be a key component of a F-actin network which interprets mechanical cues in the final stages of wing disc development, leading to Hippo pathway-mediated growth termination.

Consequently, this study also highlights the intimate and intricate connection between basic developmental mechanisms and cancer, since Tropomyosin2 appears to be necessary for normal development but also restricts uncontrolled growth. Accordingly, I showed *Drosophila* Tropomyosin2 to have a tumor suppressor function in wing discs, consistent with what was described of many HMW Tropomyosin isoforms in human cells. Not only that, but this study also suggests a possible mechanism by which the downregulation of HMW Tropomyosin isoforms contributes to cancer development.

Despite remaining elusive, the mechanism behind organ growth-termination is currently an active pursuit of many scientists. I believe that by further investigating the cytoskeletal regulation of particular Hippo pathway constituents, that mechanism can be unraveled. Not only that, but by also identifying the particular actin networks responsible for transducing cell-environment cues into signaling cascades we will come closer to a complete understanding of the beginning, middle and end of normal development. By having a more complete understanding of normal development, we will then be able to address pathologies where it is compromised in an unprecedented manner.

V Bibliography

1. Blanchoin, L. *et al.* (2014) Actin Dynamics, Architecture, and Mechanics in Cell Motility. *Physiol. Rev.* 94, 235–263

2. Pollard, T.D. and Cooper, J.A. (2009) Actin, a central player in cell shape and movement. *Science* 326, 1208–12

3. Dos Remedios, C.G. *et al.* (2003) Actin binding proteins: regulation of cytoskeletal microfilaments. *Physiol. Rev.* 83, 433–473

4. Lee, S.H. and Dominguez, R. (2010) Regulation of actin cytoskeleton dynamics in cells. *Mol. Cells* 29, 311–325

5. Taylor, M.P. *et al.* (2011) Subversion of the actin cytoskeleton during viral infection. *Nat. Rev. Microbiol.* 9, 427–39

6. Mullins R.D. (1998) The interaction of Arp2/3 complex with actin: nucleation, high affinity pointed end capping, and formation of branching networks of filaments. *PNAS* 95, 6181–6186

7. Mullins RD, Stafford WF, Pollard TD. Structure, subunit topology, and actin-binding activity of the ARP2/3 complex from Acanthamoeba Acanthamoeba. *J Cell Biol* 136: 331–343

8. Bamburg J.R. *et al.* (1980) Partial purification and characterization of an actin depolymerizing factor from brain. *FEBS Lett* 121, 178–182

9. Sellers, J.R. (2000) Myosins: a diverse superfamily. *Biochim. Biophys. Acta* 1496, 3-22

10. Khaitlina, S.Y. (2015) Tropomyosin as a Regulator of Actin Dynamics. *Int. Rev. Cell Mol. Biol.* 318, 255–291

11. Gunning, P.W. *et al.* (2008) Tropomyosin-based regulation of the actin cytoskeleton in time and space. *Physiol. Rev.* 80, 1-35

12. Gunning, P.W. *et al.* (2015) Tropomyosin - master regulator of actin filament function in the cytoskeleton. *J. Cell Sci.* 128, 2965-2974

13. Bailey, K. (1946) Tropomyosin a new asymmetric protein component of muscle. *Nature* 157, 368

14. Hitchcock-DeGregori, S. E. *et al.* (1988) Tropomyosin inhibits the rate of actin polymerization by stabilizing actin filaments. *Biochemistry* 27, 9182-9185

15. Broschat, K. O. *et al.* (1989). Tropomyosin stabilizes the pointed end of actin filaments by slowing depolymerization. *Biochemistry* 28, 8501-8506

16. Schevzov, G. *et al.* (2011) Tropomyosin isoforms and reagents. *Bioarchitecture* 1, 135–164

17. Gunning, P.W. *et al.* (2015) The evolution of compositionally and functionally distinct actin filaments. *J. Cell Sci.* 128, 2009–2019

18. Geeves, M.A. *et al.* (2015) A systematic nomenclature for mammalian tropomyosin isoforms. *J. Muscle Res. Cell Motil.* 36, 147–153

19. Lees-Miller, J.P. and Helfman, D.M. (1991) The molecular basis for tropomyosin isoform diversity. *BioEssays* 13, 429–437

20. Gunning, P.W. *et al.* (2005) Tropomyosin isoforms: Divining rods for actin cytoskeleton function. *Trends Cell Biol.* 15, 333–341

21. Sahota, V.K. *et al.* (2009) Troponin I and Tropomyosin regulate chromosomal stability and cell polarity. *J. Cell Sci.* 122, 2623–2631

22. Hsiao, J.Y. *et al.* (2015) Arp2/3 Complex and Cofilin Modulate Binding of Tropomyosin to Branched Actin Networks. *Curr. Biol.* 25, 1573–1582

23. Goins, L.M. and Mullins, R.D. (2015) A novel tropomyosin isoform functions at the mitotic spindle and Golgi in Drosophila. *Mol. Biol. Cell* 26, 2491–2504

24. Cho, A. *et al.* (2016) An Atypical Tropomyosin in Drosophila with Intermediate Filament-like Properties. *Cell Rep.* 16, 1-11

25. Vrhovski, B. *et al.* (2008) Structure and evolution of tropomyosin genes. *Adv. Exp. Med. Biol.* 644, 6–26

26. Atrrill, H. et al. The FlyBase Consortium (2016) FlyBase: establishing a Gene Group resource for Drosophila melanogaster. Rel.FB2016_05

27. McLachlan, A.D. and Stewart, M. (1975) Tropomyosin coiled-coil interactions: evidence for an unstaggered structure. *J Mol Biol* 98, 293–304

28. Wegner, A. (1979) Equilibrium of the actin-tropomyosin interaction. *J. Mol. Biol.* 131, 839-853

29. Von der Ecken, J. *et al.* (2015) Structure of the F-actin-tropomyosin complex. *Nature* 519, 114-117

30. Schevzov, G. *et al.* (2012) Functional Diversity of Actin Cytoskeleton in Neurons and its Regulation by Tropomyosin, (1st edn), 298 Elsevier Inc.

31. Blanchoin, L. *et al.* (2001) Inhibition of the Arp2/3 complex-nucleated actin polymerization and branch formation by tropomyosin. *Curr. Biol.* 11, 1300–1304

32. Bugyi, B. *et al.* (2010) How tropomyosin regulates lamellipodial actin-based motility: a combined biochemical and reconstituted motility approach. *EMBOJ.* 29, 14–26

33. Creed, S.J. *et al.* (2011) Tropomyosin isoform 3 promotes the formation of filopodia by regulating the recruitment of actin- binding proteins to actin filaments. *Exp. Cell Res.* 317, 249–261

34. Brayford, S. *et al.* (2016) Tropomyosin promotes lamellipodial persistence by collaborating with Arp2/3 at the leading edge. *Curr. Biol.* 26, 1312–1318

35. Wawro, B. *et al.* (2007) Tropomyosin regulates elongation by formin at the fast-growing end of the actin filament. *Biochemistry* 282 (11), 8435–8445

36. Tojkander, S. *et al.* (2011) A molecular pathway for myosinII recruitment to stress fibers. *Curr. Biol.* 21, 539-550

37. Huckaba, T.M. *et al.* (2006) Roles of type II myosin and a tropomyosin isoform in retrograde actin flow in budding yeast. *J. Cell Biol.* 175, 957–969

38. Ono, S. and Ono, K. (2002) Tropomyosin inhibits ADF/cofilin-dependent actin filament dynamics. *J. Cell Biol*. 156, 1065–1076

39. Lindberg, U. *et al.* (2008) Tropomyosins regulate the impact of actin binding proteins on actin filaments. *Adv. Exp. Med. Biol*. 644, 223–230

40. Helfman, D.M. *et al.* (2008) Tropomyosin as a regulator of cancer cell transformation. *Adv. Exp. Med. Biol.* 644, 124–131

41. O'Neill, G.M. *et al.* (2008) Tropomyosins as interpreters of the signaling environment to regulate the local cytoskeleton. *Semin. Cancer Biol.* 18, 35–44

42. Robertson, C.W. (1936) The metamorphosis of Drosophila melanogaster, including an accurately timed account of the principal morphological changes. *J. Morphol.* 59, 351–399

43. Beira, J. V. and Paro, R. (2016) The legacy of Drosophila imaginal discs. *Chromosoma* 125, 4, 573-592

44. Klein, T. (2001) Wing disc development in the fly: The early stages. *Curr. Opin. Genet. Dev.* 11, 470–475

45. Day, S.J. and Lawrence, P. (2000) Measuring dimensions: the regulation of size and shape. *Development* 127, 2977–87

46. Harvey, K. and Tapon, N. (2007) The Salvador-Warts-Hippo pathway [mdash] an emerging tumour-suppressor network. *Nat Rev Cancer* 7, 182–191

47. Pan, D. (2010) The hippo signaling pathway in development and cancer. *Dev. Cell* 19, 491–505

48. Halder, G. and Johnson, R.L. (2011) Hippo signaling: growth control and beyond. *Development* 138, 9–22

49. Yu, F.X. *et al.* (2015) Hippo Pathway in Organ Size Control, Tissue Homeostasis, and Cancer. *Cell* 163, 811–828

50. Zhou, D. *et al.* (2009) Mst1 and Mst2 maintain hepatocyte quiescence and suppress hepatocellular carcinoma development through inactivation of the Yap1 oncogene. *Cancer Cell* 16, 425–438

51. Zhao, B. *et al.* (2010) A coordinated phosphorylation by Lats and CK1 regulates YAP stability through SCF (beta-TRCP). *Genes Dev*. 24, 72–85

52. Zhao Li, L. *et al.* (2010) The Hippo-YAP pathway in organ size control and tumorgenesis: an updated version. *Genes Dev.* 24, 862–874

53. Halder, G. *et al.* (2012) Transduction of mechanical and cytoskeletal cues by YAP and TAZ. *Nat. Publ. Gr.* 13, 591–600

54. Sun, S. and Irvine, K.D. (2016) Cellular Organization and Cytoskeletal Regulation of the Hippo Signaling Network. *Trends Cell Biol.* xx, 1–11

55. Gaspar, P. and Tapon, N. (2014) Sensing the local environment: Actin architecture and Hippo signaling. *Curr. Opin. Cell Biol.* 31, 74–83

56. Fernández, B.G. *et al.* (2011) Actin-Capping Protein and the Hippo pathway regulate F-actin and tissue growth in Drosophila. *Development* 138, 2337–2346

57. Sansores-Garcia, L. *et al.* (2011) Modulating F-actin organization induces organ growth by affecting the Hippo pathway. *EMBO J.* 30, 2325–35

58. Gaspar, P. *et al.* (2015) Zyxin antagonizes the FERM protein expanded to couple f-actin and yorkie-dependent organ growth. *Curr. Biol.* 25, 679–689

59. Rauskolb, C. *et al.* (2014) Cytoskeletal tension inhibits Hippo signaling through an Ajuba-Warts complex. *Cell* 158, 143–156

60. Hanahan, D. and Weinberg, R.A. (2011) Hallmarks of cancer: The next generation. *Cell* 144, 646–674

61. Stehn, J.R. *et al.* (2006) Specialisation of the tropomyosin composition of actin filaments provides new potential targets for chemotherapy. *Curr Cancer Drug Targets* 6, 245–256

62. Pollack R. *et al.* (1975) Patterns of organization of actin and myosin in normal and transformed cultured cells. *PNAS* 72, 994–8

63. Yamaguchi H. and Condeelis, J. (2007) Regulation of the actin cytoskeleton in cancer cell migration and invasion. *Biochim Biophys Acta* 1773, 642– 52

64. Schevzov, G. *et al.* (2015) Regulation of cell proliferation by ERK and signal-dependent nuclear translocation of ERK is dependent on Tm5NM1-containing actin filaments. *Mol. Biol. Cell* 26, 2475–90

65. Calleja, M. *et al*. (1996) Visualization of gene expression in living adult Drosophila. *Science* 274, 252-255

66. Griffin, R. *et al.* (2014) Genetic odyssey to generate marked clones in Drosophila mosaics. *PNAS* 111, 4756–63

67. Brand, A.H. and Perrimon, N. (1993) Targeted gene expression as a means of altering cell fates and generating dominant phenotypes. *Development* 118, 401–15

68. Tanimoto, H. *et al*. (2000) Hedgehog creates a gradient of DPP activity in Drosophila wing imaginal discs. *Molecular Cell* 5, 59-71

69. Hamaratoglu, F. *et al*. (2006). The tumour-suppressor genes NF2/Merlin and Expanded act through Hippo signaling to regulate cell proliferation and apoptosis. *Nat. Cell Biol.* 8, 27-36

70. Villano, J.L. and Katz, F.N. (1995) Four-jointed is required for intermediate growth in the proximal-distal axis in Drosophila. *Development* 121, 2767-2777

71. Tanaka-Matakatsu, M. *et al*. (1996) Cadherin-mediated cell adhesion and cell motility in Drosophila trachea regulated by the transcription factor Escargot. *Development* 122, 3697–3705

72. Udan, R. S. *et al*. (2003) Hippo promotes proliferation arrest and apoptosis in the Salvador/Warts pathway. *Nat. Cell Biol.* 5, 914-920

73. Lai, Z.C. *et al*. (2005) Control of cell proliferation and apoptosis by mob as tumor suppressor, mats. *Cell* 120, 675-685

74. Roberts, D.B (1998) Drosophila, a pratical approach, *Oxford University Press*

75. Luduena RF. *(*2013) A hypothesis on the origin and evolution of tubulin. *Int Rev Cell Mol Bio*

76. Lento, W. *et al.* (2013) Wnt/Wingless Signaling in Drosophila. *Cold Spring Harb. Perspect. Biol.* 4, 6

77. Green, E.W. *et al.* (2014) A Drosophila RNAi collection is subject to dominant phenotypic effects. *Nat. Methods* 11, 222–223

78. Manning, S. *et al.* (2016) A Drosophila RNAi library modulates Hippo pathway-dependent tissue growth. *Nat. Commun.* 7, 1–6

79. Goto, A. *et al.* (2014) The chromatin regulator DMAP1 modulates activity of the nuclear factor κB (NF-κB) transcription factor Relish in the Drosophila innate immune response. *J. Biol. Chem.* 289, 20470–20476

80. Hitchcock-DeGregori, S.E. *et al.* (2007) Tropomyosin: Regulator of actin filaments. *Adv. Exp. Med. Biol.* 592, 87–97

81. Janco, M. *et al.* (2016) The impact of tropomyosins on actin filament assembly is isoform specific. *Bioarchitecture* 992, 1–15

82. Robaszkiewicz, K. *et al.* (2016) Tropomyosin isoforms differentially modulate the regulation of actin filament polymerization and depolymerization by cofilins. *FEBS J.* 283, 723–737

83. Wawro, B. *et al.* (2007) Tropomyosin regulates elongation by formin at the fast-growing end of the actin filament. *Biochemistry* 46, 8146–8155

84. Bernstein, B.W. and Bamburg, J.R. (1982) Tropomyosin binding to F-actin protects the F-actin from disassembly by brain actin-depolymerizing factor (ADF). *Cell Motil.* 2, 1–8

85. Nishida, E. *et al.* (1984) Cofilin, a protein in porcine brain that binds to actin filaments and inhibits their interactions with myosin and tropomyosin. *Biochemistry* 23, 5307–5313

86. Nakano K. and Mabuchi I. (2006) Actin-depolymerizing protein Adf1 is required for formation and maintenance of the contractile ring during cytokinesis in fission yeast. *Mol Biol Cell* 17, 1933–1945

87. Broschat, K. O. *et al.* (1989) Tropomyosin stabilizes the pointed end of actin filaments by slowing depolymerization. *Biochemistry* 28, 8501-8506

88. Bryce, N. S. *et al.* (2003) Specification of actin filament function and molecular composition by tropomyosin isoforms. *Mol. Biol. Cell* 14, 1002–1016

89. Creed, S.J. *et al.* (2011) Tropomyosin isoform 3 promotes the formation of filopodia by regulating the recruitment of actin-binding proteins to actin filaments. *Exp. Cell Res.* 317, 249–261

90. Ostap, E.M. (2008) Tropomyosins as discriminators of myosin funcation. *Adv. Exp. Med. Biol.* 644, 273–285

91. Aldaz, S. *et al.* (2013) Dual role of myosin II during Drosophila imaginal disc metamorphosis. *Nat. Commun.* 4, 1761

92. Clayton, J.E. *et al.* (2010) Differential regulation of unconventional fission yeast myosins via the actin track. *Curr. Biol.* 20, 1423–1431

93. Genevet, A. *et al.* (2009) The Hippo pathway regulates apical-domain size independently of its growth-control function. *J Cell Sci* 122, 2360–2370

94. Jezowska, B. *et al.* (2011) A dual function of Drosophila capping protein on DE-cadherin maintains epithelial integrity and prevents JNK-mediated apoptosis. *Dev. Biol.* 360, 143–159

95. Aegerter-Wilmsen, T. *et al.* (2007) Model for the regulation of size in the wing imaginal disc of Drosophila. *Mech. Dev.* 124, 318–326

96. Legoff, L. *et al.* (2013) A global pattern of mechanical stress polarizes cell divisions and cell shape in the growing Drosophila wing disc. *Development* 140, 4051–9

97. Aegerter-Wilmsen, T. *et al.* (2012) Integrating force-sensing and signaling pathways in a model for the regulation of wing imaginal disc size. *Development* 139, 3221–31

98. Buchmann, A. *et al.* (2014) Sizing it up: The mechanical feedback hypothesis of organ growth regulation. *Semin. Cell Dev. Biol.* 35, 73–81

99. Aragona, M. *et al.* (2013) A mechanical checkpoint controls multicellular growth through YAP/TAZ regulation by actin-processing factors. *Cell* 154, 1047–1059.

100. Dupont, S. *et al.* (2011) Role of YAP/ TAZ in mechanotransduction. *Nature* 474, 179–183.

101. Mateus, R. *et al.* (2015) Control of tissue growth by Yap relies on cell density and F-actin in zebrafish fin regeneration. *Development* 142, 2752–2763

102. Hergovich, A. *et al.* (2006) NDR kinases regulate essential cell processes from yeast to humans. *Nat. Rev. Mol. Cell Biol.* 7:253–264

103. Hergovich, A. (2013) Regulation and functions of mammalian LATS/NDR kinases: looking beyond canonical Hippo signalling. *Cell Biosci.* 3, 32

104. Dutta, S. and Baehrecke, E.H. (2008) Warts Is Required for PI3K-Regulated Growth Arrest, Autophagy, and Autophagic Cell Death in Drosophila. *Curr. Biol.* 18, 1466–1475

105. Emoto, K. *et al.* (2006) The tumour suppressor Hippo acts with the NDR kinases in dendritic tiling and maintenance. *Nature* 443, 210–213

106. Milán, M. *et al.* (2014) Aneuploidy and tumorigenesis in Drosophila. *Semin. Cell Dev. Biol.* 28, 110–115

Supplementary Information

S1 - Supplementary Material and Methods

Table S1 | Fly stocks used in this study

[w^- ; ;]	[w^- ; *nub*-Gal4 ; UAS-GFP]
[w^- ; ; *hh*-Gal4, UAS-GFP/TM6B]	[w^- ; *ap*-Gal4, *ex*-LacZ/CyO]
[w^- ; *nub*-Gal4, UAS-*ex*]	[w^- ; *nub*-Gal4,UAS-*wts*::Myc/CyO]
[w^- ; ; *tub*-Gal4/TM6B]	[w^- ; *fj*-LacZ/CyO, *wg*-LacZ ; *hh*-Gal4, UAS-GFP/TM6B]
[w^- ; *shg*-LacZ/CyO, *wg*-LacZ ; *hh*-Gal4, UAS-GFP/TM6B]	[w^- ; *ex*-LacZ/CyO, *wg*-LacZ ; *hh*-Gal4, UAS-GFP/MKRS]
[y^- v^- ; ; UAS-*tm2*-IR^{JF01095}]	[y^- v^- ; ; UAS-*tm2*-IR^{HMS02260}]
[w^- ; UAS-*tm2*-IR^{KK111307}]	[w^- ; UAS-mCherry]
[w^- ; IF/CyO ; MKRS/TM6B]	[w^- ; UAS-RFP/CyO ; MKRS/TM6B]
[w^- ; IF/CyO ; UAS-*tm2*-IR^{JF}/TM6B]	[w^- ; UAS-RFP/CyO ; UAS-*tm2*-IR^{JF}/TM6B]

S1.1   Molecular biology and sequencing

To confirm the presence of the correct RNAi hairpin in both TRiP RNAi fly lines (*tm2*-IR^{JF} and *tm2*-IR^{HMS}), genomic DNA was extracted using a genomic DNA isolation protocol: 6 male flies are collected in Eppendorf tubes and flash-frozen (-80ºC); frozen flies are ground in 200µl of buffer A (100mM Tris-HCl, pH 7.5; 100mM EDTA; 100mM NaCl; 0.5% SDS); an additional 200µl of buffer A is added and flies are ground until only cuticles remain; Eppendorf tubes are incubated for 30min at 65ºC; 800µl of LiCl/KAc solution (5M KAc stock + 6M LiCl stock at 1:2,5 ratio) is added to the Eppendorf tubes; tubes are left incubating on ice for at least 10min; 15min spin (max RPM) and discard supernatant; wash with 70% EtOH (500µl) and dry pellet; re-suspend pellet in 150µl nuclease free H2O (Sigma).

Extracted gDNA was used for PCR following instructions of the manufacturer (Promega GoTaq DNA Polymerase kit) with slight changes in thermal cycling conditions (Initial denaturation – 95ºC for 4min; 30 cycles – 95ºC for 30s, 49ºC for 30s, 72ºC for 30s; Final extension – 72ºC for 10min; Soak – 12ºC). For each RNAi line, I used primers recommended by the TRiP (*tm2*-IR^{JF} – Fwd: 5'ACCAGCAACCAAGTAAATCAAC3', Rev: 5'GATTTCACACAGATCAGCCG3'; *tm2*-IR^{HMS} – Fwd: 5'ACCAGCAACCAAGTAAATCAAC3', Rev: 5'GGTAGGCATCACACACGATTA3'). Fragment size was verified by agarose gel electrophoresis (1,5% agarose, TAE1x, RedSafe 1:100000; 100v), where GeneRuler 1kb DNA Ladder (ThermoFisher Scientific) was used to estimate fragment size. The fragments amplified from the *tm2*-IR^{JF} fly line were prepared for sequencing using BigDye Terminator v1.1 Cycle Sequencing Protocol (ThermoFisher Scientific) and sent to the IGC Genomics unit for sequencing.

The sequence was then analyzed using FichTV software to correct possible sequence errors and compared to the sequence of one arm of TRiP JF01095 dsRNAi available on Flybase.org. Sequence comparison was done using Nucleotide BLAST (NCBI NIH).

S2 - Supplementary Results

S2.1   RNAi construct identity confirmation

A PCR from genomic DNA (gDNA) extracts of each fly line was carried out to confirm the identity of the RNAi construct inserted in each fly line (Fig.S1a). Because the *tm2*-IR[JF01095] and the *tm2*-IR[HMS02260] TRiP RNAi constructs were engineered using the VALIUM1 and VALIUM20 plasmids, respectively. I therefore designed primers that targeted regions surrounding one dsRNAi arm in each plasmid. The primer pairs that would amplify the dsRNAi insertion in the JF01095 and HMS02260 VALIUM plasmids should amplify a band at 574bp and 339bp, respectively. As a control, I used a PCR reaction with no gDNA (Fig.S1a, lane1). The size of amplified product was in agreement with what was expected from the used primer pairs. Moreover, PCR product from the *tm2*-IR[JF01095] line was sequenced and aligned against the sequence of one arm of TRiP *tm2*-IR[JF01095] dsRNAi (Flybase.org). The product amplified from the *tm2*-IR[JF01095] fly line was 98% identical to its respective hairpin arm with a BLAST score of 734bits (Fig.S1b). All together, these results indicate that the *tm2*-IR[JF01095] and *tm2*-IR[HMS02260] TRiP RNAi flies have the correct RNAi insert.
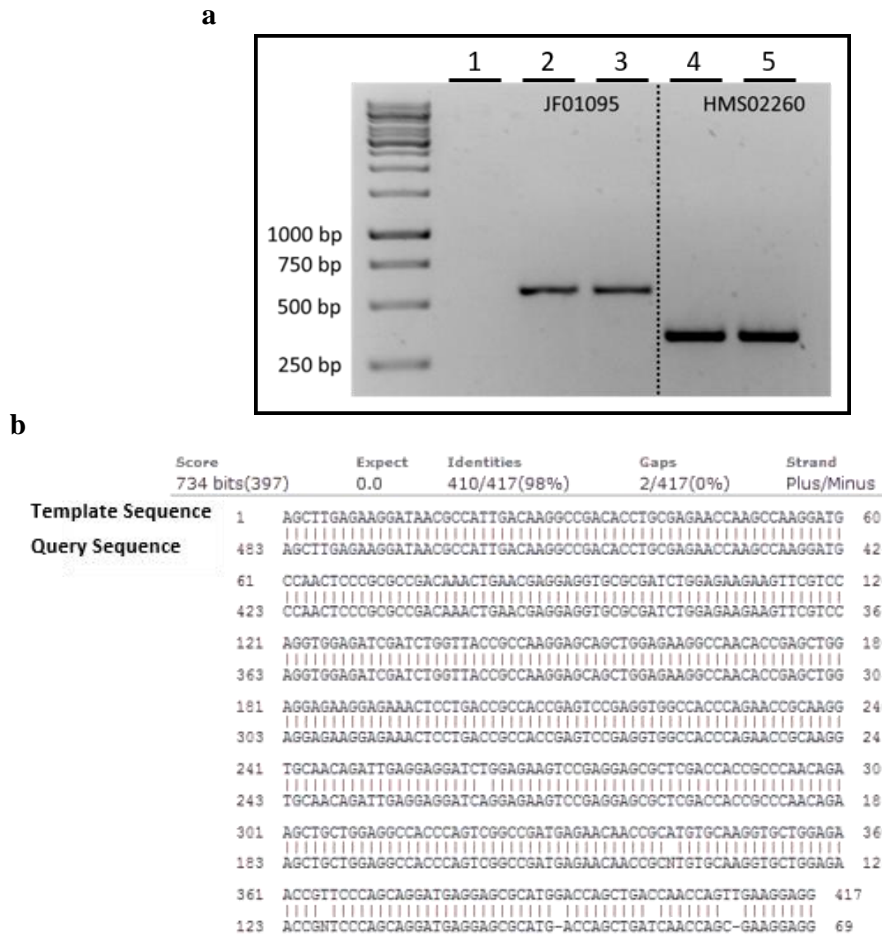
a

b

Figure S1 | TRiP RNAi lines have the correct hairpin size and sequence

a – Agarose gel loaded with PCR reactions; lane 1 – PCR reagents with no gDNA (negative control); lanes 2 & 3 – *tm2*-IR[JF01095] gDNA, amplified with the *tm2*-IR[JF] Fwd and Rev primer pairs; lanes 4 & 5 – *tm2*-IR[HMS] gDNA, amplified with the tm2-IR[HMS] Fwd and Rev primer pairs; **b –** Nucleotide alignment of JF01095 sequenced hairpin arm**; template sequence** – *tm2*-IR[JF01095] dsRNAi arm sequence available on Flybase.org; **query sequence**-sequencing result.

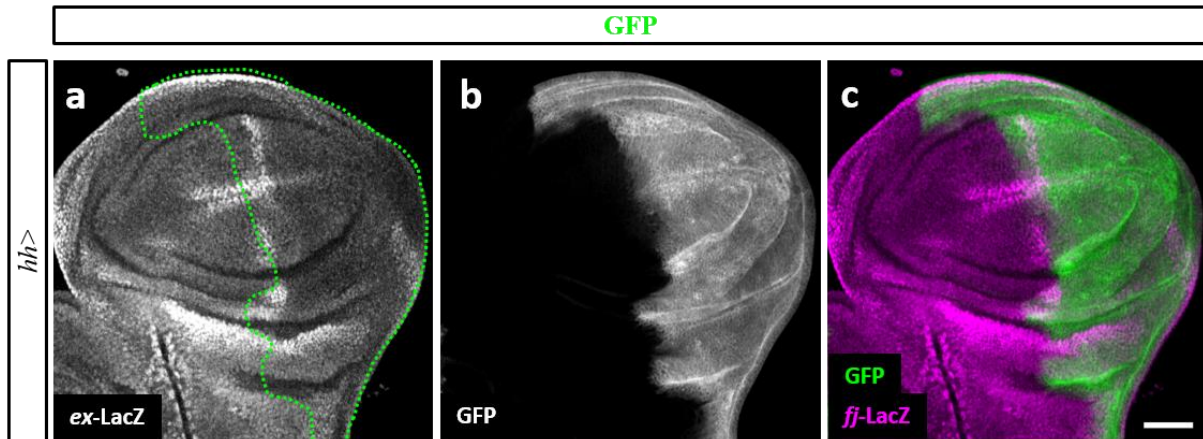### S2.2   *shotgun* expression upon *tm2* downregulation

Figure S2 | Control *shg*-LacZ expression

All panels display wing imaginal discs from 3rd instar *Drosophila* larvae**. a-c –** Standard confocal projections. **a-c –** *hh*-Gal4 driving UAS-*GFP* in discs carrying *shg*-LacZ. Posterior domain is marked by GFP expression (**b** – white; **c** - green); discs are stained with α-β-Galactosidase to highlight LacZ reporters (**a**– white; **c** - magenta). Green dotted lines outline GFP-expressing domains (**a**) Scale bar=40μm (**a-c**).

S2.3   Exon Composition of Human and *Drosophila* Tropomyosins is Comparable

This study stems from the observation that human TPM2 is downregulated in pre-malignant breast tumor samples and in an inducible cancer cell line that mimics the stages of cancer progression. In a subsequent screen, *Drosophila tm2* was found to have a role in preventing wing disc overgrowth. Therefore, I wondered whether findings from studying the role of *Drosophila* Tropomyosins in growth could be extrapolated to human Tropomyosins and cancer. To do this, I compared the exon composition and sequence of Tropomyosin genes between *Drosophila* and Humans (Fig.S3). In this analysis, I compared the sequence of all coding exons of human Tropomyosin genes (TPM1, TPM2, TPM3 and TPM4) to the sequence of each *Drosophila* Tropomyosin gene. Exons with a max score of at least 15 and at least 35% identity were taken into account, though they were considered marginally similar (Fig.S3, checkered boxes) while exons were considered similar if their alignment had a max score of 20 or greater and over 50% identity (Fig.S3, full boxes).

This analysis covered the exon composition of the tropomyosin genes because most, if not all, isoforms are generated by alternative splicing of said exons. Also, a similar analysis has already been performed where exon sequence of mammals, birds, amphibians and fish tropomyosin genes was compared[16]. Even though I considered the possibility of *tm1* and *tm2* contributing to different vertebrate tropomyosins, very few exons had exclusive contribution from either *tm1* or *tm2*. TPM exon 9d, for instance, only had similarities with *tm2* exon 3 and while TPM exon 1b was only marginally similar to a portion of *tm2* exon1, it had a much higher amount of similarity to exon 7 of *tm1* (Fig.S3a,c,d).

Another interesting finding was that while exon structure in the tropomyosin genes was completely different between *Drosophila* and humans, there was a sequential equivalence between the amino acid sequence, regardless of exons. The strongest conservation between the exons of the different species was from the non-variable exons which are present in all Tpm isoforms, exons 3,4,5,7 and 8. Additionally, this analysis uncovered that *tm2* exon 4 had no any similarities with any human exon (Fig.S3).

With this analysis alone, we were not able to determine a clear and distinguishable contribution of *tm2* towards a particular human tropomyosin gene unfortunately. However, *tm2* isoforms are more comparable to human HMW tropomyosin isoforms than LMW ones because all LMW TPM isoforms have exon1b, which has only a low degree of similarity with *tm2,* especially when compared to *tm1*.
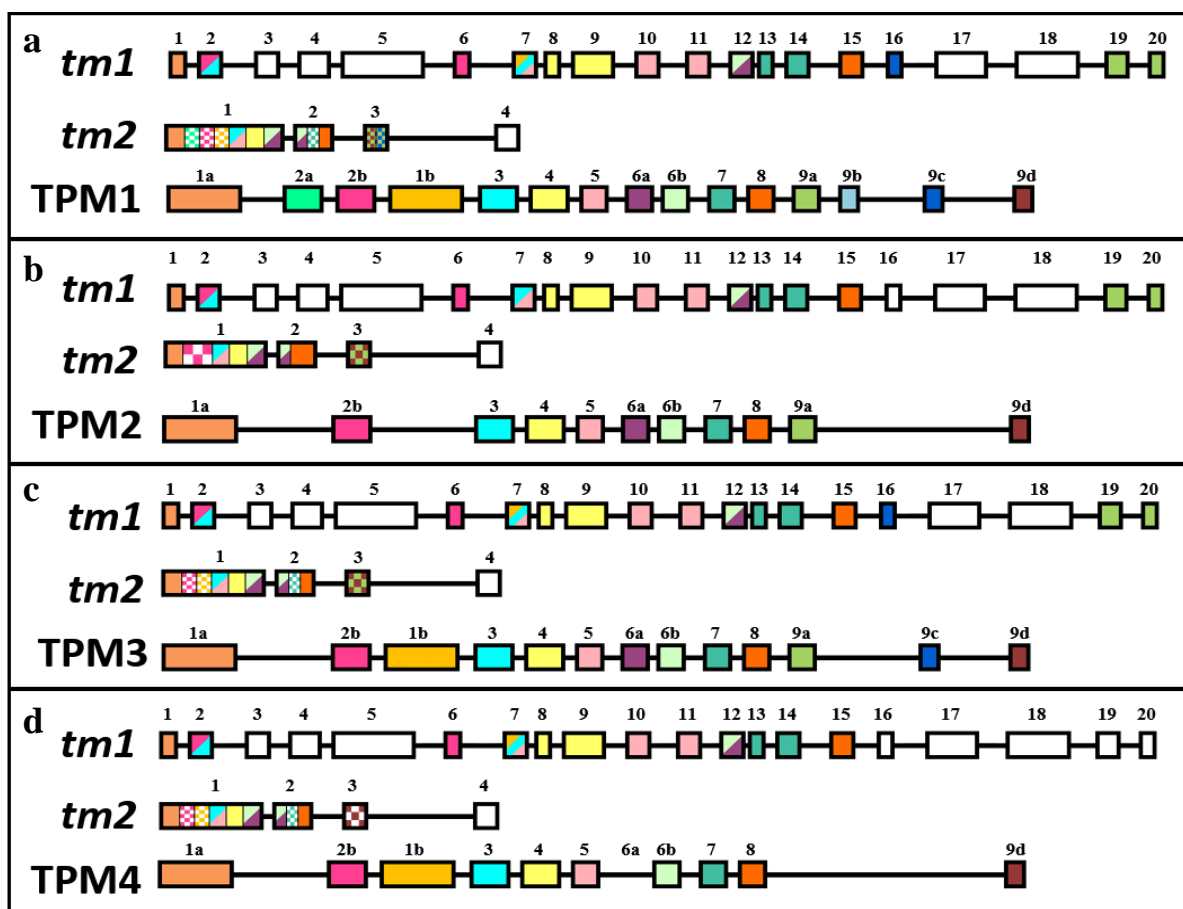

Figure S3 | Both *tm1* and *tm2* contribute to every human Tropomyosin exon

a-d – Coding-exon schematic of *Drosophila* (*tm1* and *tm2*) and human (TPM1, TPM2, TPM3 and TPM4) Tropomyosin genes; *tm1* and *tm2* exons are colored according to their similarity to TPM1 (**a**), TPM2 (**b**), TPM3 (**c**) and TPM4 (**d**) exons. **a** – Exon comparison between *Drosophila* Tropomyosins and TPM1. **b** – Exon comparison between *Drosophila* Tropomyosins and TPM2. **c** – Exon comparison between *Drosophila* Tropomyosins and TPM3. **d** - Exon comparison between *Drosophila* Tropomyosins and TPM4. White boxes – exons with no similarity to human TPM exons. Exons were considered similar with a BLAST max score of ≥20 and identity ≥50% (full-colored boxes) and marginally similar with a BLAST max score of ≥15 and identity ≥35% (checkered-colored boxes).